

Weierstraß-Institut
für Angewandte Analysis und Stochastik
Leibniz-Institut im Forschungsverbund Berlin e. V.

Preprint

ISSN 0946 – 8633

**Convergence of an implicit Voronoi finite volume method for
reaction-diffusion problems**

André Fiebach¹, Annegret Glitzky¹, Alexander Linke¹

submitted: August 12, 2013

¹ Weierstrass Institute
Mohrenstr. 39
10117 Berlin
Germany
email: andre.fiebach@wias-berlin.de
annegret.glitzky@wias-berlin.de
alexander.linke@wias-berlin.de

No. 1827
Berlin 2013



2010 *Mathematics Subject Classification.* 35K57, 35R05, 65M08, 65M12, 80A30.

Key words and phrases. reaction-diffusion systems; heterostructures; finite volume method; convergence; long-term simulation.

A. Fiebach was partially supported by the European Commission within the *Seventh Framework Programme (FP7)* MD³ "Material Development for Double Exposure and Double Patterning".

A. Linke (project D27) and A. Glitzky (project D22) are partially supported by the DFG Research Center MATHEON *Mathematics for key technologies*.

The authors would like to thank Klaus Gärtner and Jens André Griepentrog for their assistance and for valuable discussions.

Edited by
Weierstraß-Institut für Angewandte Analysis und Stochastik (WIAS)
Leibniz-Institut im Forschungsverbund Berlin e. V.
Mohrenstraße 39
10117 Berlin
Germany

Fax: +49 30 20372-303
E-Mail: preprint@wias-berlin.de
World Wide Web: <http://www.wias-berlin.de/>

Abstract

We investigate the convergence of an implicit Voronoi finite volume method for reaction-diffusion problems including nonlinear diffusion in two space dimensions. The model allows to handle heterogeneous materials and uses the chemical potentials of the involved species as primary variables. The numerical scheme uses boundary conforming Delaunay meshes and preserves positivity and the dissipative property of the continuous system. Starting from a result on the global stability of the scheme (uniform, mesh-independent global upper and lower bounds), we prove strong convergence of the chemical activities and their gradients to a weak solution of the continuous problem. In order to illustrate the preservation of qualitative properties by the numerical scheme, we present a long-term simulation of the Michaelis-Menten-Henri system. Especially, we investigate the decay properties of the relative free energy and the evolution of the dissipation rate over several magnitudes of time, and obtain experimental orders of convergence for these quantities.

1 Introduction and model equations

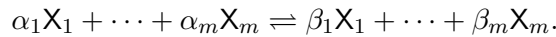
In a bounded domain $\Omega \subset \mathbb{R}^2$ we consider m species X_ν with initial densities U_ν which undergo diffusion processes and undergo chemical reactions. The relation between the densities u_ν of the species X_ν and the corresponding chemical potentials v_ν is assumed to be given by Boltzmann statistics, i.e.,

$$u_\nu = \bar{u}_\nu e^{v_\nu}, \quad \nu = 1, \dots, m. \quad (1.1)$$

The reference densities \bar{u}_ν may depend on the spatial position and express the possible heterogeneity of the system under consideration. For the mass fluxes j_ν we make the ansatz

$$j_\nu = -D_\nu(\cdot, e^{v_1}, \dots, e^{v_m}) u_\nu \nabla v_\nu, = -D_\nu \bar{u}_\nu e^{v_\nu} \nabla v_\nu, \quad \nu = 1, \dots, m, \quad (1.2)$$

with diffusion coefficients $D_\nu : \Omega \times \mathbb{R}^m \rightarrow \mathbb{R}_+$ which are allowed to depend on the space variable and the state variable. To describe chemical reactions we introduce a finite subset $\mathcal{R} \subset \mathbb{Z}_+^m \times \mathbb{Z}_+^m$. Each pair $(\vec{\alpha}, \vec{\beta}) \in \mathcal{R}$ represents the vectors of stoichiometric coefficients of a reversible reaction, written in the form



According to the mass action law, the net rate of such a pair of reactions is of the form $k_{(\vec{\alpha}, \vec{\beta})} (a^{\vec{\alpha}} - a^{\vec{\beta}})$, where $k_{(\vec{\alpha}, \vec{\beta})}$ is a reaction coefficient, $a_\nu := \exp(v_\nu)$ corresponds to the chemical activity of X_ν , and

$a^\alpha := \prod_{\nu=1}^m a_\nu^{\alpha_\nu}$. The net production rate of species X_ν corresponding to all accruing reactions is

$$R_\nu(\cdot, e^{v_1}, \dots, e^{v_m}) := \sum_{(\alpha, \beta) \in \mathcal{R}} k_{(\alpha, \beta)} (a^\alpha - a^\beta) (\beta_\nu - \alpha_\nu). \quad (1.3)$$

The stoichiometric subspace \mathcal{S} is defined by

$$\mathcal{S} = \text{span}\{\alpha - \beta : (\alpha, \beta) \in \mathcal{R}\}$$

and its orthogonal complement is denoted by \mathcal{S}^\perp . Our reaction-diffusion system consists of m continuity equations. Considering no flux boundary conditions on $\Gamma = \partial\Omega$ we obtain the following system of partial differential equations:

$$\begin{aligned} \frac{\partial u_\nu}{\partial t} + \nabla \cdot j_\nu - R_\nu &= 0 \text{ in } \mathbb{R}_+ \times \Omega, & \mathbf{n} \cdot j_\nu &= 0 \text{ on } \mathbb{R}_+ \times \Gamma, \\ u_\nu(0) &= U_\nu \text{ in } \Omega, & \nu &= 1, \dots, m. \end{aligned} \quad (1.4)$$

The aim of the paper consists in a study of a discretization scheme (Euler backward in time and Voronoi finite volume meshes in space) of Problem (1.4). It is strongly desired to retain the analytic properties of the continuous problem also in the discretization scheme.

For the introduced nonlinear reaction-diffusion system we prove the convergence of the discretized solutions to a weak solution of the continuous problem for arbitrary, even anisotropic boundary conforming Delaunay-Voronoi finite volume meshes. Basic ingredients are energy estimates and uniform strictly positive lower and upper bounds for the discretized densities as proven in [8].

Convergence studies of discretization schemes for nonlinear PDEs are an ongoing research topic. In [7] the convergence of a reaction-diffusion system including the fast reaction limit is studied. The work of [1] proves convergence of a nonlinear degenerate chemotaxis model. Furthermore, in [6] the convergence of a gradient scheme for nonlinear parabolic equations is demonstrated.

In Section 2 we collect the general assumptions concerning the data of the continuous problem and give a summary on results obtained so far for the continuous problem. Section 3 starts with the description of the discretization, introduces the prolonged quantities, summarizes results obtained so far for the discrete scheme and gives some uniqueness result for the discrete problem. Our main results concerning the convergence of the scheme are proved in Section 4. We start with a-priori estimates in Subsection 4.1 from which we derive in Subsection 4.2 the existence of a converging subsequence and prove that the limit is a weak solution of the continuous problem. Finally we derive strong convergence results. The paper is closed by a numerical example involving the Michaelis-Menten-Henri kinetics. Besides the concentrations of the different species, we investigate the decay properties of the relative free energy and the evolution of the dissipation rate, and obtain experimental orders of convergence for these quantities. In Appendix A we collect some results needed in Section 4.

2. The continuous problem

2.1. General assumptions on the data

We formulate basic assumptions with respect to the data of the problem, cf. [15, 11].

Definition 2.1 (Reaction order, cf. [11]). A source term of a reaction is of order n , iff there exists a smallest number $n \in \mathbb{N}$ such that there exists a constant $c > 0$ with

$$\begin{aligned} \max_{\nu=1, \dots, m} \left\{ (\beta_\nu - \alpha_\nu) (a^\alpha - a^\beta) \right\} &\leq c \left(1 + \sum_{\nu=1}^m a_\nu^n \right) \\ \forall a \in \mathbb{R}_+^m, \forall (\alpha, \beta) \in \mathcal{R}. \end{aligned} \quad (2.5)$$

We study the problem under the following assumptions:

(A1) $\Omega \subset \mathbb{R}^2$ is a *bounded polygonal domain*, $\Gamma := \partial\Omega$.

Let $m \in \mathbb{N}$ be given and \mathcal{R} a finite subset of $\mathbb{Z}_+^m \times \mathbb{Z}_+^m$. For all $(\alpha, \beta) \in \mathcal{R}$ the reaction rates $k_{(\alpha, \beta)} : \Omega \times \mathbb{R}^m \rightarrow \mathbb{R}_+$ satisfy the *Carathéodory condition* and there exist real constants $0 < \underline{c}_k, \bar{c}_k < \infty$ such that $\underline{c}_k \leq k_{(\alpha, \beta)}(\mathbf{x}, \mathbf{y}) \leq \bar{c}_k$, f.a.a. $\mathbf{x} \in \Omega, \forall \mathbf{y} \in \mathbb{R}^m$. Source terms of reactions are at most quadratic.

The diffusion coefficients $D_\nu : \Omega \times \mathbb{R}^m \rightarrow \mathbb{R}_+$ satisfy the *Carathéodory condition* and there exist constants $0 < \underline{c}_D, \bar{c}_D < \infty$ such that $\underline{c}_D \leq D_\nu(\mathbf{x}, \mathbf{y}) \leq \bar{c}_D$, f.a.a. $\mathbf{x} \in \Omega, \forall \mathbf{y} \in \mathbb{R}^m$ and $\nu = 1, \dots, m$. Finally, $\bar{u}_\nu, U_\nu \in L^\infty(\Omega)$ and there exist constants $0 < \underline{c}_{\bar{u}}, \bar{c}_{\bar{u}} < \infty$ and $0 < \underline{c}_U, \bar{c}_U < \infty$ such that $\underline{c}_{\bar{u}} \leq \bar{u}_\nu(\mathbf{x}) \leq \bar{c}_{\bar{u}}$, and $\underline{c}_U \leq U_\nu(\mathbf{x}) \leq \bar{c}_U$, resp. f.a.a. $\mathbf{x} \in \Omega$ and $\nu = 1, \dots, m$.

Remark 2.2. These technical assumptions (A1) allow us to handle a general class of reaction-diffusion systems, including heterogeneous materials and nonlinear diffusion processes. Heterogeneous materials can be found quite often in the modeling of biological or chemical processes involving different phases (see [3]). Therefore, we assume the dependence of the diffusion coefficients and the reaction rate coefficients on the spatial variable. For example, a different state of matter or a different background material leads to coefficients which are spatially dependent in a maybe non smooth way.

The dependence of the diffusion coefficients on the state variable is motivated by problems like those considered in [10, 9]. For example, recombination reactions of Shockley-Read-Hall, Auger type, and mole fractions, see [11, 33, 21, 14], contain reaction rate coefficients depending on the state variable. Sometimes enzymes have more than one binding side where the reactivity of a docking place is influenced by the number of free bindings (in biochemistry the behavior is called allosteric regulation). From the modeling point of view this leads to reaction coefficients which depend on the concentration of an regulating molecule, see [26].

The assumptions on the space dimension and on the reaction order are technical to obtain existence and boundedness results in a general class of problems as in [11] for the continuous problem. Note, that only the source terms of the reaction terms are restricted, the sink terms may be large.

2.2. Summary of results for the continuous problem

Let $u := (u_1, \dots, u_m), v := (v_1, \dots, v_m)$ and $a := (a_1, \dots, a_m)$ denote the vector of densities, chemical potentials and activities of all species. Let us introduce the Gelfand triple $X \in Y \cong Y^* \in X^*$, where

$$X := H^1(\Omega, \mathbb{R}^m), \quad Y := L^2(\Omega, \mathbb{R}^m), \quad W := X \cap L^\infty(\Omega, \mathbb{R}^m).$$

Moreover, we define the operators $A : W \rightarrow X^*, E : X \rightarrow X^*$ by

$$\begin{aligned} \langle Av, \bar{v} \rangle &:= \int_{\Omega} \left(\sum_{\nu=1}^m D_\nu \bar{u}_\nu e^{v_\nu} \nabla v_\nu \cdot \nabla \bar{v}_\nu - R_\nu(e^v) \bar{v}_\nu \right) dx, \\ \langle Ev, \bar{v} \rangle &:= \sum_{\nu=1}^m \int_{\Omega} (\bar{u}_\nu e^{v_\nu} \bar{v}) dx \quad \forall \bar{v} \in X. \end{aligned} \tag{2.6}$$

In the setting of (A1), a weak formulation of (1.4) can be stated as follows: Find (u, v) such that:

$$\left. \begin{aligned} u'(t) + Av(t) &= 0, \quad u(t) = Ev(t) \text{ f.a.a. } t \in \mathbb{R}_+, \quad u(0) = U, \\ u &\in H_{\text{loc}}^1(\mathbb{R}_+, X^*), \quad v \in L_{\text{loc}}^2(\mathbb{R}_+, X) \cap L^\infty(\mathbb{R}_+, L^\infty(\Omega, \mathbb{R}^m)). \end{aligned} \right\} \tag{P}$$

Such problems have been investigated e.g. in [20, 15]; the papers [11, 12, 17, 18, 19] deal with electrically charged species. The papers [11, 12, 16, 17] consider more general state equations than (1.1). We shortly summarize results for (P) obtained in two space dimensions.

If (u, v) is a solution to (P) then

$$u(t) - U \in \mathcal{U} := \left\{ w \in X^* : \left(\langle w_\nu, \mathbf{1} \rangle \right)_{\nu=1, \dots, m} \in \mathcal{S} \right\} \quad \forall t > 0. \tag{2.7}$$

Therefore, if $u^* := \lim_{t \rightarrow \infty} u(t)$ exists, then necessarily $u^* \in U + \mathcal{U}$. According to [11, 17] there exists a unique stationary solution (u^*, v^*) to (P) additionally fulfilling $u^* \in U + \mathcal{U}$. This (u^*, v^*) is a thermodynamic equilibrium of the system. The free energy along solutions to (P) decays monotonously and exponentially to its equilibrium value [16, 20].

If the source terms of all reactions are of maximal order 2 then all solutions (u, v) to (P) are globally bounded, especially the particle densities are positively bounded away from zero (see e.g. [19]).

Considering regularized problems, finding a priori estimates which do not depend on the regularization level, and solving the regularized problems the existence of solutions to (P) is shown in [19, 11]. Uniqueness results for (P) can be obtained by standard arguments, if the diffusion coefficients do not depend on the state variables. For cases with diffusion coefficients depending on the state variable we refer to [11]. In three space dimensions there are similar, but weaker results available, see [20, 11].

3. Discretized reaction-diffusion systems

3.1. Voronoi finite volume discretization

The solutions of reaction-diffusion systems preserve some quantities like mass (invariants, cf. (2.7)) and positivity. Therefore, the aim is to respect the conservation of these quantities by the approximated solution. The finite volume method has been developed by engineers to study systems of conservation laws.

In the following, we work with Voronoi meshes, which represent a class of admissible finite volume meshes [5]. In the following, we will assume that the Voronoi meshes \mathcal{M} are derived as dual grids of boundary conforming Delaunay triangulations \mathcal{T} . The Delaunay grids will be used for piecewise affine interpolation by P_1 finite element functions.

Our notation is basically taken from [15] and visualized in Figure 1.

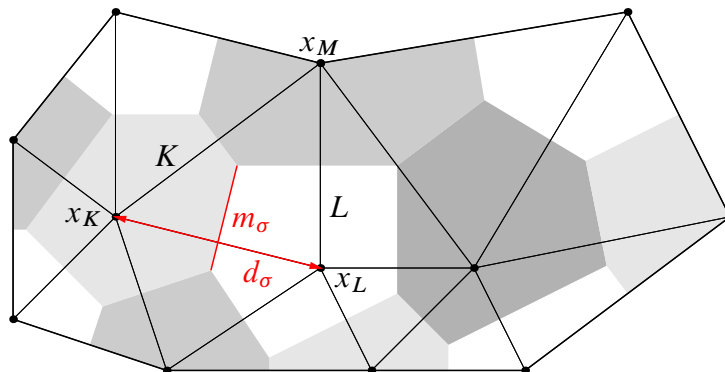


Figure 1: Notation of Voronoi meshes $\mathcal{M} = (\mathcal{P}, \mathcal{V}, \mathcal{E})$

Let Ω be an open bounded, polygonal subset of \mathbb{R}^2 . A Voronoi mesh is defined as triple $\mathcal{M} = (\mathcal{P}, \mathcal{V}, \mathcal{E})$. Here, \mathcal{P} denotes a family of *grid points* in $\bar{\Omega}$, \mathcal{V} denotes a family of *Voronoi control volumes* and \mathcal{E} denotes a family of *faces* in \mathbb{R} . The number of grid points is denoted by $M = \#\mathcal{P}$.

The corresponding control volume K of each grid point $x_K \in \mathcal{P}$ is defined by

$$K = \{x \in \Omega : |x - x_K| < |x - x_L| \quad \forall x_L \in \mathcal{P}, x_L \neq x_K\}.$$

The set of all neighboring control volumes of K is denoted by $\mathcal{N}_{\mathcal{V}}(K)$. The Lebesgue measure of each control volume K is denoted by $|K|$ and the mesh size of \mathcal{M} by

$$\text{size}(\mathcal{M}) = \sup_{K \in \mathcal{V}} \text{diam}(K).$$

For two different $K, L \in \mathcal{V}$ the one-dimensional Lebesgue measure of $\bar{K} \cap \bar{L}$ is either zero or $\bar{K} \cap \bar{L} = \bar{\sigma}$ for one $\sigma \in \mathcal{E}$. Here the symbol $\sigma = K|L$ denotes the one-dimensional face between the control volumes K and L and m_{σ} is its Lebesgue measure.

We introduce the subset $\mathcal{E}_{int} \subset \mathcal{E}$ containing all interior faces. Further, we introduce for all $K \in \mathcal{V}$ the subset $\mathcal{E}_K \subset \mathcal{E}_{int}$, such that $\forall \sigma \in \mathcal{E}_K \exists L \in \mathcal{N}_{\mathcal{V}}(K) : \sigma = \bar{L} \cap \bar{K}$.

The Euclidian distance between two neighboring grid points $x_K, x_L \in \mathcal{P}$ over the face $\sigma = K|L \in \mathcal{E}_{int}$ is denoted by d_σ .

Remark 3.1 (see [15]). Let $\mathcal{M} = (\mathcal{P}, \mathcal{V}, \mathcal{E})$ a Voronoi mesh. The dual $(\mathcal{P}, \mathcal{T})$ of a Voronoi mesh consists of a family \mathcal{P} of *grid points* in $\bar{\Omega}$ and a family \mathcal{T} of triangles and is called *Delaunay triangulation* if any circumcircle of a triangle $T = (x_K, x_L, x_M) \in \mathcal{P}^3$ does not contain any vertex $x_J \in \mathcal{P}$ with $x_J \notin T$. A Delaunay triangulation is called *boundary conforming* iff the circumcircles of all triangles with $T \cap \partial\Omega \neq \emptyset$ do not contain any grid point $x_J \in \mathcal{P}$, $x_J \notin T$.

A Voronoi mesh is derived from a Delaunay triangulation by the intersection of half spaces and hence convex. If the domain consists of more than one material and the interfaces are aligned to the triangle edges of the Delaunay mesh, then all subdomain triangulations have to be boundary conforming.

Definition 3.2 (see [13]). Let Ω be an open bounded, polygonal subset of \mathbb{R}^2 and $\mathcal{M} = (\mathcal{P}, \mathcal{V}, \mathcal{E})$ a Voronoi mesh.

- The symbol $X_{\mathcal{V}}(\mathcal{M})$ denotes the set of all piecewise constant functions from Ω to \mathbb{R} which are constant on every Voronoi control volume $K \in \mathcal{V}$. The constant value of $w_h \in X_{\mathcal{V}}(\mathcal{M})$ on the control volume $K \in \mathcal{V}$ is denoted by w_K .
- Let $p \geq 1$. The discrete L^p -norm of $w_h \in X_{\mathcal{V}}(\mathcal{M})$ is defined by

$$\|w_h\|_{L^p} = \left(\sum_{K \in \mathcal{V}} |K| |w_K|^p \right)^{1/p}.$$

- The discrete H^1 semi-norm of $w_h \in X_{\mathcal{V}}(\mathcal{M})$ is defined by

$$|w_h|_{H^1, \mathcal{M}}^2 = \sum_{\sigma=K|L \in \mathcal{E}_{int}} T_\sigma |w_K - w_L|^2, \quad T_\sigma := \frac{m_\sigma}{d_\sigma}.$$

Here w_K and w_L are the constant values of w_h in the control volumes K and L . The term T_σ is the so called transmissibility across the edge $\sigma = K|L$, see [5]. The full discrete H^1 -norm is given by

$$\|w_h\|_{H^1, \mathcal{M}}^2 = |w_h|_{H^1, \mathcal{M}}^2 + \|w_h\|_{L^2}^2.$$

We prescribe the approximation of a function $f : \Omega \times \mathbb{R}^m \rightarrow \mathbb{R}$ by

$$f_K(\cdot) := \frac{1}{|K|} \int_K f(x, \cdot) dx,$$

where $K \in \mathcal{V}$. In this context we introduce the approximation of the diffusion coefficients and the reaction terms on a Voronoi cell $K \in \mathcal{V}$ by

$$D_{\nu K}(\cdot) = \frac{1}{|K|} \int_K D_\nu(x, \cdot) dx, \quad R_{\nu K}(\cdot) = \frac{1}{|K|} \int_K R_\nu(x, \cdot) dx, \quad (3.8)$$

and analogously the approximation of $k_{(\alpha, \beta)K}$.

The corresponding piecewise constant function can be estimated from above and below by the upper and lower bound of the continuous function. For $K \in \mathcal{V}$ we denote by

$$u_\nu^{(K)} = \int_K u_\nu(x) dx = |K| u_{\nu K} = \bar{u}_{\nu K} e^{v_{\nu K}} |K|, \quad \bar{u}_{\nu K} = \frac{1}{|K|} \int_K \bar{u}_\nu(x) dx$$

the mass of the ν -th species in K and by $u_{\nu K}$ the constant density on K . For every species X_ν , $\nu = 1, \dots, m$, we introduce the discrete initial values by

$$U_\nu^{(K)} := \int_K U_\nu(x) dx, \quad K \in \mathcal{V}.$$

The space-discrete version of the continuous problem (P) is obtained by testing with the characteristic function of K . Using Gauss theorem, we derive the approximated flux term

$$\int_K \nabla \cdot \mathbf{j}_\nu dx = \int_{\partial K} \mathbf{j}_\nu \cdot \mathbf{n}_K d\Gamma \approx \sum_{\sigma=K|L \in \mathcal{E}_K} -T_\sigma Y_\nu^\sigma Z(v_{\nu L}, v_{\nu K})(v_{\nu L} - v_{\nu K}),$$

where

$$Z(x, y) = \begin{cases} \frac{e^x - e^y}{x - y}, & \text{for } x \neq y, \\ e^x, & \text{for } x = y, \end{cases} \quad x, y \in \mathbb{R}, \quad (3.9)$$

represents the logarithmic mean value of e^x in the interval $[x, y]$. In the following we write $Z_\nu^\sigma = Z(v_{\nu L}, v_{\nu K})$ for $\sigma = K|L \in \mathcal{E}_{int}$ and $D_{\nu K} = D_{\nu K}(e^{v_{1K}}, \dots, e^{v_{mK}})$. With this definition of Z_ν^σ it is possible to switch between a gradient in potentials and activities, i.e. the discrete version of $\nabla a_\nu = a_\nu \nabla v_\nu$ holds. The symbol Y_ν^σ defines an averaging of $D_\nu \bar{u}_\nu$ over the edge $\sigma = K|L$, which is symmetric in K and L , and is given by

$$Y_\nu^\sigma = \frac{D_{\nu K} + D_{\nu L}}{2} \frac{\bar{u}_{\nu K} + \bar{u}_{\nu L}}{2}, \quad \sigma = K|L.$$

By $D_{\nu K}$ we mean $D_{\nu K} = D_{\nu K}(e^{v_{1K}}, \dots, e^{v_{mK}})$. Following [15], we use the notation

$$\begin{aligned} \mathbf{u}_\nu &= (u_\nu^{(K)})_{K \in \mathcal{V}}, & \mathbf{u} &= (\mathbf{u}_1, \dots, \mathbf{u}_m), & \mathbf{u}_K &= (u_{\nu K})_{\nu=1}^m, \\ \mathbf{v}_\nu &= (v_{\nu K})_{K \in \mathcal{V}}, & \mathbf{v} &= (\mathbf{v}_1, \dots, \mathbf{v}_m), & \mathbf{v}_K &= (v_{\nu K})_{\nu=1}^m, \\ \mathbf{U}_\nu &= (U_\nu^{(K)})_{K \in \mathcal{V}}, & \mathbf{U} &= (\mathbf{U}_1, \dots, \mathbf{U}_m), \\ \mathbf{a}_K &= (e^{v_{\nu K}})_{\nu=1}^m, & \mathbf{a}_\nu &= (e^{v_{\nu K}})_{K \in \mathcal{V}}, & \nu &= 1, \dots, m. \end{aligned}$$

Furthermore, we define the scalar products

$$\langle \mathbf{u}_\nu, \mathbf{v}_\nu \rangle_{\mathbb{R}^M} = \sum_{K \in \mathcal{V}} |K| u_{\nu K} v_{\nu K}, \quad \langle \mathbf{u}, \mathbf{v} \rangle_{\mathbb{R}^{Mm}} = \sum_{\nu=1}^m \langle \mathbf{u}_\nu, \mathbf{v}_\nu \rangle_{\mathbb{R}^M}.$$

Definition 3.3 (Time discretization). Let $S = [0, T] \subset \mathbb{R}_+$ be a finite time interval. A time discretization of S is defined as a strictly increasing sequence of real numbers $(t_n)_{n=1}^N$ with $t_0 = 0$ and $t_N = T$. The time step is defined by

$$t_\delta^{(n)} = t_n - t_{n-1} < \infty \quad \text{for } n = 1, \dots, N$$

and the largest possible time step is denoted by $\bar{t}_{\delta N} = \sup_{n=1, \dots, N} t_\delta^{(n)}$.

A discretization of the whole domain $Q = S \times \Omega$ is defined by the tuple $\mathcal{D} = (\mathcal{M}, (t_n)_{n=1}^N)$ and the size of the discretization is denoted by $\text{size}(\mathcal{D}) = \max\{\text{size}(\mathcal{M}), \bar{t}_{\delta N}\}$. In the convergence proof we consider $\text{size}(\mathcal{D}) \rightarrow 0$. We introduce the operator $\hat{E} : \mathbb{R}^{Mm} \rightarrow \mathbb{R}^{Mm}$ by

$$\hat{E}\mathbf{v} = \left((\bar{u}_{\nu K} e^{v_{\nu K}} |K|)_{\nu=1, \dots, m} \right)_{K \in \mathcal{V}},$$

which maps in every control volume the chemical potential of every species to its mass. Furthermore we define $\hat{A} : \mathbb{R}^{Mm} \rightarrow \mathbb{R}^{Mm}$ by

$$\hat{A}\mathbf{v} = \left(\sum_{\sigma=K|L \in \mathcal{E}_K} -T_\sigma Y_\nu^\sigma Z_\nu^\sigma (v_{\nu L} - v_{\nu K}) - |K| R_{\nu K}(e^{v_{\nu K}}) \right)_{\substack{K \in \mathcal{V}, \\ \nu=1, \dots, m}}. \quad (3.10)$$

Using these definitions we state the discrete version of (P) by: Find a tuple (\mathbf{u}, \mathbf{v}) such that

$$\left. \begin{aligned} \frac{\mathbf{u}(t_n) - \mathbf{u}(t_{n-1})}{t_\delta^{(n)}} + \widehat{A}\mathbf{v}(t_n) &= \mathbf{0}, \quad \mathbf{u}(t_n) = \widehat{E}\mathbf{v}(t_n), \quad n = 1, \dots, N \\ \mathbf{u}(0) &= \mathbf{U}. \end{aligned} \right\} \quad (P_{\mathcal{D}})$$

The discrete weak form of \widehat{A} is given by

$$\begin{aligned} \langle \widehat{A}\mathbf{v}, \mathbf{w} \rangle_{\mathbb{R}^{Mm}} &= \sum_{\nu=1}^m \sum_{\sigma=K|L \in \mathcal{E}_{int}} T_\sigma Y_\nu^\sigma Z_\nu^\sigma (v_{\nu L} - v_{\nu K})(w_{\nu L} - w_{\nu K}) \\ &\quad - \sum_{\nu=1}^m \sum_{K \in \mathcal{V}} |K| R_{\nu K} (e^{\mathbf{v}_K}) w_{\nu K} \quad \forall \mathbf{v}, \mathbf{w} \in \mathbb{R}^{Mm}. \end{aligned} \quad (3.11)$$

We associate the discrete (vectorial) solutions (\mathbf{u}, \mathbf{v}) to $(P_{\mathcal{D}})$ piecewise constant functions (u_h, v_h) and call them solutions to $(P_{\mathcal{D}})$, too.

Remark 3.4. In all proofs, real constants $C > 0$ with different meaning are numbered consecutively. The constants only depend on the data (lower bounds of the diffusion coefficients, upper bounds of the reaction rate constants, lower and upper bounds of the reference densities and initial values), see (A1) and not on the discretization, unless otherwise stated.

Concerning vectors $\mathbf{w} \in \mathbb{R}^k$, $k \in \mathbb{N}$ we use: By writing $\mathbf{w} \geq \mathbf{0}$ we mean $w_i \geq 0$ resp. $w_i > 0$ for $i = 1, \dots, k$. By $\ln \mathbf{w}$ we denote $(\ln w_i)_{i=1}^k$, and by $e^{\mathbf{w}}$ the vector $(e^{w_i})_{i=1}^k$ is denoted.

Moreover the symbols S_1 , S_2 and S_3 have a local meaning and differ from time to time. Generally these terms arise from testing the problem $(P_{\mathcal{D}})$ by test functions and discussing the expressions for the time-derivative (S_1), diffusion term (S_2) and reaction term (S_3) separately.

3.2. Prolongated quantities

We introduce piecewise constant in time and piecewise constant in space interpolation of \mathbf{a}_ν denoted by $a_{\nu,h}(t, x)$ fulfilling $a_{\nu,h}(t, x) = a_{\nu K}(t_n)$ for $t \in (t_{n-1}, t_n]$ and $x \in K$, $K \in \mathcal{V}$. By $a_{\nu,l}(t, x)$ we denote the piecewise constant in time and piecewise linear in space interpolation of \mathbf{a}_ν fulfilling $a_{\nu,l}(t, x_K) = a_{\nu K}(t_n)$ for $t \in (t_{n-1}, t_n]$ and $K \in \mathcal{V}$. Writing a_l we mean $a_l = (a_{\nu,l})_{\nu=1}^m$ and by a_h we mean $a_h = (a_{\nu,h})_{\nu=1}^m$. The same notation holds for the chemical potentials \mathbf{v}_ν . Further we introduce an operator $K_{\mathcal{D}}$ mapping the space-time-discrete concentrations into the space $C(S, X^*)$ by

$$(K_{\mathcal{D}}u_h)(t) := \frac{1}{t_\delta^{(n)}} ((t - t_{n-1})u_h(t_n) + (t_n - t)u_h(t_{n-1})) \quad \text{for } t \in (t_{n-1}, t_n].$$

We remark that the concentrations u_h are piecewise constant on the control volumes $K \in \mathcal{V}$. Obviously, it holds $(K_{\mathcal{D}}u_h)' = \frac{1}{t_\delta^{(n)}} (u_h(t_n) - u_h(t_{n-1}))$ for all $t \in (t_{n-1}, t_n]$. With e^{v_l} we denote the vector $(e^{v_{\nu,l}})_{\nu=1}^m$.

We introduce a reconstruction of the reference densities onto the grid by $\widehat{P}_{\mathcal{D}}\bar{u}_{\nu,h}$. For this we work with the half-diamonds

$$\begin{aligned} T_{\sigma K} &= \{tx_K + (1-t)y : t \in (0, 1), y \in \sigma\}, \\ T_{\sigma L} &= \{tx_L + (1-t)y : t \in (0, 1), y \in \sigma\}, \end{aligned}$$

where $\sigma = K|L \in \mathcal{E}$ denotes the Voronoi surface of two neighboring Voronoi cells K , L with corresponding nodes x_K , $x_L \in \mathcal{P}$, see Figure 2. The two half-diamonds $T_{\sigma K}$ and $T_{\sigma L}$ form the so-called kite $D_\sigma = T_{\sigma K} \cup T_{\sigma L}$ of the edge $\sigma = K|L \in \mathcal{E}_{int}$, the union of all these kites covers the domain Ω . Then the reconstruction operator is defined by

$$\widehat{P}_{\mathcal{D}}\bar{u}_{\nu,h}(x) = \begin{cases} \bar{u}_{\nu K}, & \text{if } x \in T_{\sigma K}, \\ \bar{u}_{\nu L}, & \text{if } x \in T_{\sigma L} \end{cases} \quad \forall \sigma = K|L \in \mathcal{E}. \quad (3.12)$$

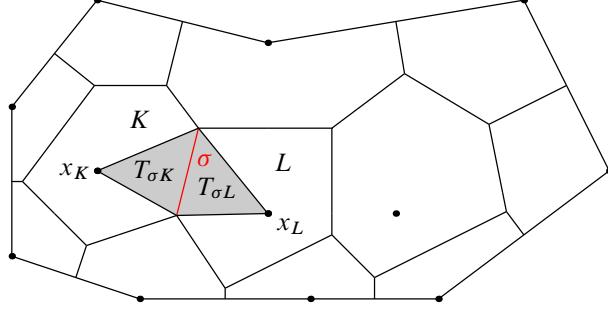


Figure 2: Kite $D_\sigma = T_{\sigma K} \cup T_{\sigma L}$ of the edge $\sigma = K|L$.

We use the piecewise constant in space interpolation of the discretized reaction term $R_{\nu K}$ and the discretized diffusion coefficient $D_{\nu K}$ introduced by $R_{\nu,h}(x, a_h(x)) = R_{\nu,K}(\mathbf{a}_K)$ and by $D_{\nu,h}(x, a_h(x)) = D_{\nu,K}(\mathbf{a}_K)$ for all $x \in K$, $K \in \mathcal{V}$, see (3.8). In the same manner as in (3.12) we denote the reconstruction operator of the diffusion coefficient by $(\widehat{P}_{\mathcal{D}} D_{\nu,h}(a_h))(x)$. Note that the same L^∞ -bounds for the diffusion coefficient and the reference densities given in (A1), also hold for its reconstruction $\widehat{P}_{\mathcal{D}} \bar{u}_{\nu h}$ and $\widehat{P}_{\mathcal{D}} D_{\nu,h}(a_h)$. Since

$$\widehat{P}_{\mathcal{D}} \bar{u}_{\nu h}(x) = \bar{u}_{\nu K} = \bar{u}_{\nu h}(x), \quad x \in T_{K|L}, L \in \mathcal{N}_{\mathcal{V}}(K), K \in \mathcal{V}$$

we can write shortly $\bar{u}_{\nu h}$ instead of $\widehat{P}_{\mathcal{D}} \bar{u}_{\nu h}$. The same holds for $(\widehat{P}_{\mathcal{D}} D_{\nu,h}(a_h))(x)$ and therefore we write $D_{\nu,h}(a_h)$.

3.3. Summary of results for the discretized problem

We collect some results for the discrete problem. For more details we refer to our previous papers [15, 8]. In [8] it was proved that the discrete problem $(P_{\mathcal{D}})$ has a local solution, if we assume for the reaction terms that the following sensible conditions

$$R_\nu(\cdot, (a_1, \dots, a_{\nu-1}, 0, a_{\nu+1}, \dots, a_m)) \geq 0 \quad \forall \nu = 1, \dots, m, \mathbf{a} \in \mathbb{R}_+^m, \quad (3.13)$$

and

$$\exists \mathbf{s}^\perp \in \mathcal{S}^\perp : \mathbf{s}^\perp > \mathbf{0} \quad (3.14)$$

hold, see [8, (3.14)] and [8, (3.15)]. Condition (3.13) is known as quasi positivity, see [2, 28]. The second condition (3.14) imposes conservation of atom number, see [14, Sec. 6.4.3]. As stated in [8, 15] the solutions u_h of the discrete problem $(P_{\mathcal{D}})$ lie in an affine subspace $U + \widehat{\mathcal{U}}$ and there exists a unique stationary solution to $(P_{\mathcal{D}})$.

We work with boundary conforming Delaunay-Voronoi meshes and impose the additional assumption on the reference densities:

- (A2) Let \mathcal{I} be a finite index set. Let $\Omega \subset \mathbb{R}^2$ be a polygonal domain and let $\Omega = \cup_{I \in \mathcal{I}} \Omega_I$ be a finite disjoint union of subdomains such that the discontinuities of \bar{u}_ν , $\nu = 1, \dots, m$, coincide with subdomain boundaries. Let the over all one dimensional measure of all internal subdomain boundaries be bounded by θ . There exists some $\gamma \in (0, 1]$ such that $\bar{u}_\nu \in C^{0,\gamma}(\Omega_I) := \{w|_{\Omega_I}, w \in C^{0,\gamma}(\mathbb{R}^2)\}$, $\nu = 1, \dots, m, I \in \mathcal{I}$, see [15, (A4)].

For all $R > 0$ exists a constant $\gamma_R \in (0, 1]$ such that $k_{(\boldsymbol{\alpha}, \boldsymbol{\beta})}|_{\Omega_I} \in C^{0,\gamma_R}(\Omega_I \times \mathcal{B}_{\mathbb{R}^m}(0, R))$ for all $(\boldsymbol{\alpha}, \boldsymbol{\beta}) \in \mathcal{R}$ and $D_\nu|_{\Omega_I} \in C^{0,\gamma_R}(\Omega_I \times \mathcal{B}_{\mathbb{R}^m}(0, R))$, $\nu = 1, \dots, m$ for all $I \in \mathcal{I}$. Here $\mathcal{B}_{\mathbb{R}^m}(0, R)$ denotes the ball in \mathbb{R}^m centered at 0 with radius R .

Moreover, there exists a constant $P \in \mathbb{N}$ such that for all considered discretizations $\mathcal{D} = (\mathcal{M}, (t_n)_{n=1}^N)$ of $\Omega \times S$ the property $\sup_{\mathcal{M}=(\mathcal{P}, \mathcal{V}, \mathcal{E})} \max_{K \in \mathcal{V}} \text{card } \mathcal{E}_K \leq P$ holds.

Along all solutions (\mathbf{u}, \mathbf{v}) to $(P_{\mathcal{D}})$ the free energy

$$\widehat{F}(\mathbf{u}) = \sum_{\nu=1}^m \sum_{K \in \mathcal{V}} |K| \left(u_{\nu K} \left(\ln \frac{u_{\nu K}}{\bar{u}_{\nu K}} - 1 \right) + \bar{u}_{\nu K} \right)$$

decays monotonously and exponentially to its equilibrium value, see [15]. For all $\mathbf{v} \in \mathbb{R}^{Mm}$ the dissipation rate of the system is given by $D(\mathbf{v}) := \left\langle \widehat{A}\mathbf{v}, \mathbf{v} \right\rangle_{\mathbb{R}^{Mm}}$ and nonnegative, see [15].

The next result supplies the main ingredient for our new results.

Theorem 3.5 (Uniform upper and lower bounds, see [8, Theorem 3, 4]). *Let (A1) be fulfilled and $\mathcal{D} = (\mathcal{M}, (t_n)_{n=1}^N)$ be a discretization fulfilling (A2). Then there exist constants $0 < c_1, c_2 < \infty$ only depending on the data and not on the mesh size of \mathcal{M} such that for every solution (u_h, v_h) to $(P_{\mathcal{D}})$*

$$\operatorname{ess\,inf}_{x \in \Omega} u_{\nu, h}(t_n) \geq c_1 \quad \forall n \geq 1, \quad \nu = 1, \dots, m \quad (3.15a)$$

$$\operatorname{ess\,sup}_{x \in \Omega} u_{\nu, h}(t_n) \leq c_2 \quad \forall n \geq 1, \quad \nu = 1, \dots, m \quad (3.15b)$$

holds uniformly for all discretizations.

From Theorem 3.5 we conclude for $\nu = 1, \dots, m$

$$0 < \operatorname{inf\,ess\,inf}_{\mathcal{D}} \operatorname{inf}_{x \in \Omega} a_{\nu, h}(t), \quad \operatorname{sup\,ess\,sup}_{\mathcal{D}} \operatorname{sup}_{x \in \Omega} a_{\nu, h}(t) < \infty \quad \forall t \in S. \quad (3.16)$$

3.4. Uniqueness result

In this subsection we prove the uniqueness of the discrete solution. Only for this result we additionally assume that the diffusion coefficients only depend on the space variable and not on the state variable. The results in the other sections are independent of this assumption.

Theorem 3.6. *Let (A1) be fulfilled and $\mathcal{D} = (\mathcal{M}, (t_n)_{n=1}^N)$ a discretization fulfilling (A2). Assuming that the diffusion coefficients only depend on the space variable and not on the state variable and suppose that the time step restriction*

$$t_{\delta}^{(n)} < \frac{c_{\bar{u}}}{2C_2} \quad \forall n = 1, \dots, N \quad (3.17)$$

holds, where C_2 depends on the Lipschitz constant of the reactions. Then there exists at most one solution to the discrete problem $(P_{\mathcal{D}})$.

Proof. It suffices to prove uniqueness on a time step t_{n-1} to t_n . Assuming that $(P_{\mathcal{D}})$ has two solutions $(\mathbf{u}(t_n), \mathbf{v}(t_n))$ and $(\widehat{\mathbf{u}}(t_n), \widehat{\mathbf{v}}(t_n))$ for the same initial value $(\mathbf{u}(t_{n-1}), \mathbf{v}(t_{n-1}))$. We test $(P_{\mathcal{D}})$ by the difference of the two solutions $\tilde{\mathbf{a}} = \mathbf{e}^{\mathbf{v}} - \mathbf{e}^{\widehat{\mathbf{v}}}$. From (3.11) we deduce $S_1 + S_2 = S_3$ with

$$\begin{aligned} S_1 &:= \left\langle \frac{\mathbf{u}(t_n) - \mathbf{u}(t_{n-1})}{t_{\delta}^{(n)}}, \tilde{\mathbf{a}}(t_n) \right\rangle_{\mathbb{R}^{Mm}} - \left\langle \frac{\widehat{\mathbf{u}}(t_n) - \widehat{\mathbf{u}}(t_{n-1})}{t_{\delta}^{(n)}}, \tilde{\mathbf{a}}(t_n) \right\rangle_{\mathbb{R}^{Mm}} \\ &= \left\langle \frac{\tilde{\mathbf{u}}(t_n) - \tilde{\mathbf{u}}(t_{n-1})}{t_{\delta}^{(n)}}, \tilde{\mathbf{a}}(t_n) \right\rangle_{\mathbb{R}^{Mm}} \end{aligned}$$

and

$$\begin{aligned} S_2 &:= \sum_{\nu=1}^m \sum_{\sigma=K | L \in \mathcal{E}_{int}} T_{\sigma} Y_{\nu}^{\sigma} ((a_{\nu L} - a_{\nu K}) - (\widehat{a}_{\nu L} - \widehat{a}_{\nu K})) (\tilde{a}_{\nu L} - \tilde{a}_{\nu K}) \\ S_3 &:= \sum_{\nu=1}^m \sum_{K \in \mathcal{V}} |K| (R_{\nu K}(\mathbf{a}_K) - R_{\nu K}(\widehat{\mathbf{a}}_K)) \tilde{a}_{\nu K}. \end{aligned}$$

Since the diffusion coefficients only depend on the space variable, the averaging Y_ν^σ is equal for both solutions. Since $(x - y)x \geq \frac{1}{2}(x^2 - y^2)$ and $\|\tilde{a}_{\nu,h}(t_{n-1})\|_{L^2}^2 = 0$ the term S_1 can be estimated by

$$S_1 \geq \sum_{\nu=1}^m \frac{1}{t_\delta^{(n)}} \left\{ \frac{\underline{c}_{\bar{u}}}{2} \|\tilde{a}_{\nu,h}(t_n)\|_{L^2}^2 - \frac{\bar{c}_{\bar{u}}}{2} \|\tilde{a}_{\nu,h}(t_{n-1})\|_{L^2}^2 \right\} = \frac{\underline{c}_{\bar{u}}}{2t_\delta^{(n)}} \|\tilde{a}_h(t_n)\|_Y^2.$$

By (A1) the flux term S_2 can be estimated with a constant $C_1 > 0$ as follows

$$S_2 = \sum_{\nu=1}^m \sum_{\sigma \in \mathcal{E}_{int}} T_\sigma Y_\nu^\sigma (\tilde{a}_{\nu L} - \tilde{a}_{\nu K})^2 \geq \underline{c}_D \underline{c}_{\bar{u}} \sum_{\nu=1}^m |\tilde{a}_{\nu,h}|_{H^1, \mathcal{M}}^2.$$

Due to Theorem 3.5 and the local Lipschitz continuity of the reaction terms we find with $C_2 > 0$

$$|S_3| \leq \sum_{\nu=1}^m \sum_{K \in \mathcal{V}} |K| |R_{\nu K}(\mathbf{a}_K) - R_{\nu K}(\hat{\mathbf{a}}_K)| \|\tilde{\mathbf{a}}\| \leq C_2 \sum_{\nu=1}^m \|\tilde{a}_{\nu,h}\|_{L^2}^2.$$

The constant C_2 depends on the Lipschitz constant of the reaction term. From $S_1 + S_2 = S_3$ we find

$$\sum_{\nu=1}^m \left\{ \underline{c}_{\bar{u}} \left(\frac{1}{2t_\delta^{(n)}} - \frac{C_2}{\underline{c}_{\bar{u}}} \right) \|\tilde{a}_{\nu,h}\|_{L^2}^2 + \underline{c}_D \underline{c}_{\bar{u}} |\tilde{a}_{\nu,h}|_{H^1, \mathcal{M}}^2 \right\} \leq 0.$$

The assumption (3.17) ensures that the term in front of the L^2 -norm is greater zero. Hence $\tilde{a}_{\nu,h} = 0$ for all $n = 1, \dots, N$ and $\nu = 1, \dots, m$ and the two solutions coincide. \square

4. Convergence

4.1. A priori estimates

In a first step we provide uniform bounds for the solutions to the discrete problem $(P_{\mathcal{D}})$ for different discretization levels.

Lemma 4.1 (A priori estimates). *Let (A1) be fulfilled and let $\mathcal{D} = (\mathcal{M}, (t_\delta^n)_{n=1}^N)$ be a sequence of discretizations fulfilling (A2). For solutions (u_h, v_h) to the discrete Problems $(P_{\mathcal{D}})$ the reconstructed quantities a_l and $K_{\mathcal{D}} u_h$ fulfill*

$$\sup_{\mathcal{D}} \left\{ \|a_l\|_{L^2(S, X)} + \|K_{\mathcal{D}} u_h\|_{H^1(S, X^*)} + \|K_{\mathcal{D}} u_h\|_{C(S, Y)} \right\} < +\infty.$$

Proof. We test the discrete Problem $(P_{\mathcal{D}})$ with $\mathbf{a}(t_n)$. By using the inequality $1/2(x^2 - y^2) \leq (x - y)x$ for $x, y \in \mathbb{R}_+$, the lower and upper bounds on the reference densities, see (A1), we obtain the following estimate

$$\begin{aligned} S_1 &:= \sum_{n=1}^N t_\delta^{(n)} \left\langle \frac{\mathbf{u}(t_n) - \mathbf{u}(t_{n-1})}{t_\delta^{(n)}}, \mathbf{a}(t_n) \right\rangle_{\mathbb{R}^{Mm}} \\ &\geq \sum_{\nu=1}^m \left(\frac{\underline{c}_{\bar{u}}}{2} \|a_{\nu,h}(t_N)\|_{L^2}^2 - \frac{\bar{c}_{\bar{u}}}{2} \|a_{\nu,h}(0)\|_{L^2}^2 \right). \end{aligned}$$

On the other hand by using the definition of \hat{A} and Z_ν^σ as well as Theorem 3.5 we get from (3.11) the estimate

$$\begin{aligned} S_1 &= - \sum_{n=1}^N t_\delta^{(n)} \left\langle \hat{A} \mathbf{v}(t_n), \mathbf{a}(t_n) \right\rangle_{\mathbb{R}^{Mm}} \\ &\leq \sum_{\nu=1}^m \sum_{n=1}^N t_\delta^{(n)} \left\{ -c_1 \|a_{\nu,h}\|_{H^1, \mathcal{M}}^2 + c_1 \|a_{\nu,h}\|_{L^2}^2 + c_2 \right\}. \end{aligned}$$

Here c_1 is a positive constant depending on the lower bound of the reference densities and the diffusion coefficients. The reaction term was estimated by by some constant due to Theorem 3.5. The discrete H^1 semi-norm was completed to the full H^1 norm. Therefore we deduce using Theorem 3.5 once more with constants $c_3, c_4 > 0$

$$\begin{aligned} \sup_{\mathcal{D}} \|a_l\|_{L^2(S,X)}^2 &\leq \sup_{\mathcal{D}} \left\{ \sum_{n=1}^N t_\delta^{(n)} \sum_{\nu=1}^m \|a_{\nu,h}\|_{H^1,\mathcal{M}}^2 \right\} \\ &\leq \sup_{\mathcal{D}} \sum_{\nu=1}^m \left\{ c_3 \|a_{\nu,h}(0)\|_{L^2}^2 + c_4 \sum_{n=1}^N t_\delta^{(n)} (\|a_{\nu,h}\|_{L^2}^2 + 1) \right\} < \infty. \end{aligned} \quad (4.18)$$

From Theorem 3.5 we also conclude

$$\sup_{\mathcal{D}} \sup_{t \in S} \|u_h(t)\|_Y = \sup_{\mathcal{D}} \sup_{t \in S} \|K_{\mathcal{D}} u_h(t)\|_Y < \infty$$

and $\sup_{\mathcal{D}} \|K_{\mathcal{D}} u_h\|_{L^2(S,Y)} < \infty$. Since $K_{\mathcal{D}}$ is a continuous interpolant in time we find $K_{\mathcal{D}} u_h \in C(S, Y)$ and $\sup_{\mathcal{D}} \|K_{\mathcal{D}} u_h\|_{C(S,Y)} < \infty$. We prove the boundedness of

$$\sup_{\mathcal{D}} \|(K_{\mathcal{D}} u_h)'\|_{L^2(S,X^*)}^2 = \sup_{\mathcal{D}} \sum_{n=1}^N \int_{t_{n-1}}^{t_n} \|(K_{\mathcal{D}} u_h)'\|_{X^*}^2 dt. \quad (4.19)$$

First we estimate $\|(K_{\mathcal{D}} u_h)'(t)\|_{X^*}^2$. For this we use an arbitrary $w \in X$ and denote by $w_{\nu K} = \frac{1}{|K|} \int_K w_{\nu}(x) dx$ for all $K \in \mathcal{V}$ and $\nu = 1, \dots, m$. By w_h we denote the corresponding piecewise constant function. Then we obtain

$$\begin{aligned} \left| \left\langle \frac{u_h(t_n) - u_h(t_{n-1})}{t_\delta^{(n)}}, w \right\rangle_{X^*} \right| &= \left| \left\langle u_h(t_n) - u_h(t_{n-1}), \frac{w}{t_\delta^{(n)}} \right\rangle_Y \right| \\ &= \left| \sum_{\nu=1}^m \sum_{K \in \mathcal{V}} |K| \frac{u_{\nu K}(t_n) - u_{\nu K}(t_{n-1})}{t_\delta^{(n)}} w_{\nu K} \right| \\ &= \left| \left\langle \frac{\mathbf{u}(t_n) - \mathbf{u}(t_{n-1})}{t_\delta^{(n)}}, \mathbf{w} \right\rangle_{\mathbb{R}^{Mm}} \right| \\ &= \left| \left\langle \widehat{A} \mathbf{v}(t_n), \mathbf{w} \right\rangle_{\mathbb{R}^{Mm}} \right| \end{aligned}$$

Using (3.11), (3.9), the boundedness of the reaction terms due to (A1), by Theorem 3.5 and Hölders inequality we obtain the following estimates

$$\left| \left\langle \widehat{A} \mathbf{v}, \mathbf{w} \right\rangle_{\mathbb{R}^{Mm}} \right| \leq \sum_{\nu=1}^m \left\{ c_5 |a_{\nu,h}|_{H^1,\mathcal{M}} |w_{\nu,h}|_{H^1,\mathcal{M}} + c_6 \|w_{\nu,h}\|_{L^2} \right\}.$$

Using the following arguments

- $|w_{\nu,h}|_{H^1,\mathcal{M}} \leq C \|w_{\nu}\|_{H^1(\Omega)}$, see [5, Lemma 3.4];
- $\|w_{\nu,h}\|_{L^2} \leq C \|w_{\nu}\|_{H^1} + \|w_{\nu} - w_{\nu,h}\|_{L^2}$;
- by a discrete Poincaré inequality (see [8, (A.38)]) results

$$\begin{aligned} \|w_{\nu} - w_{\nu,h}\|_{L^2(\Omega)}^2 &= \sum_{K \in \mathcal{V}} \|w_{\nu} - w_{\nu K}\|_{L^2(K)}^2 \\ &\leq C \text{diam}(\Omega)^2 \sum_{K \in \mathcal{V}} \|w_{\nu}\|_{H^1(K)}^2 = C \text{diam}(\Omega)^2 \|w_{\nu}\|_{H^1(\Omega)}^2, \end{aligned}$$

and we get

$$\left| \langle \widehat{A}\mathbf{v}, \mathbf{w} \rangle_{\mathbb{R}^{Mm}} \right| \leq \left(c_7 \sum_{\nu=1}^m |a_{\nu,h}|_{H^1, \mathcal{M}} + c_8 \right) \|w\|_X.$$

Thus we find

$$\|(K_{\mathcal{D}}u_h)'\|_{X^*}^2 \leq \left(c_7 \sum_{\nu=1}^m |a_{\nu,h}|_{H^1, \mathcal{M}} + c_8 \right)^2$$

and by using $\|a_l\|_{L^2(S, X)} < \infty$ we obtain from (4.19) the following estimate

$$\sup_{\mathcal{D}} \sum_{n=1}^N \int_{t_{n-1}}^{t_n} \|(K_{\mathcal{D}}u_h)'\|_{X^*}^2 dt \leq \sup_{\mathcal{D}} c_9 \int_S \left(\sum_{\nu=1}^m |a_{\nu,h}|_{H^1, \mathcal{M}}^2 + 1 \right) dt < \infty$$

for all \mathcal{D} . Finally, together with $\sup_{\mathcal{D}} \|K_{\mathcal{D}}u_h\|_{L^2(S, X^*)} \leq c_{10} \sup_{\mathcal{D}} \|K_{\mathcal{D}}u_h\|_{L^2(S, Y)} < \infty$ we obtain $\sup_{\mathcal{D}} \|K_{\mathcal{D}}u_h\|_{H^1(S, X^*)} < \infty$. \square

4.2. Weak solution

In this subsection we prove that a subsequence of solutions to the discrete problems ($P_{\mathcal{D}}$) converges to a weak solution of the continuous problem (P). In a first step we show the weak convergence of subsequences in different spaces and by using a result of [23] we obtain strong convergence of a subsequence of the chemical activities in $L^2(S, Y)$. In a second step we conclude the strong convergence of the chemical activities in $L^2(S, X)$.

Theorem 4.2. *Let (A1) be fulfilled and let $\mathcal{D} = (\mathcal{M}, (t_{\delta}^n)_{n=1}^N)$ be a sequence of discretizations fulfilling (A2). Then there exist $\widehat{a} \in L^\infty(S, Y) \cap L^2(S, X)$, $\widehat{u} \in H^1(S, X^*) \cap L^2(S, Y)$ and non-labeled subsequences a_h, a_l, u_h such that*

$$a_h \rightarrow \widehat{a} \text{ in } L^2(S, Y), \quad a_l \rightarrow \widehat{a} \text{ in } L^2(S, X), \quad (4.20)$$

$$u_h \rightarrow \widehat{u} \text{ in } L^2(S, Y), \quad K_{\mathcal{D}}u_h \rightharpoonup \widehat{u} \text{ in } H^1(S, X^*) \quad (4.21)$$

as $\text{size}(\mathcal{D}) \rightarrow 0$. And $(\widehat{u}, \widehat{v}) = (\widehat{u}, \ln \widehat{a})$ is a weak solution of the continuous problem (P).

Have in mind, that the sequence of reference densities is bounded from above and below, i.e. there exist $0 < \underline{c}_{\bar{u}} \leq \bar{c}_{\bar{u}} < \infty$ such that

$$\underline{c}_{\bar{u}} \leq \min_{\nu=1, \dots, m} \text{ess inf}_{x \in \Omega} \bar{u}_{\nu, h}(x) \leq \bar{u}_{\nu, h} \leq \max_{\nu=1, \dots, m} \text{ess sup}_{x \in \Omega} \bar{u}_{\nu, h}(x) \leq \bar{c}_{\bar{u}},$$

see also (A1).

Proof. In order to show the assertions of the theorem we proceed in several steps.

Weak Precompactness: Due to Lemma 4.1 and (3.16) we deduce the existence of functions

$$\widehat{a} \in L^\infty(S, Y) \cap L^2(S, X), \quad \widehat{u} \in H^1(S, X^*) \cap L^2(S, Y),$$

such that, at least for non-labeled subsequences,

1. $\bar{u}_h \rightarrow \bar{u}$ in Y ,
2. $a_l \rightharpoonup \widehat{a}$ in $L^2(S, X), L^2(S, Y)$,
3. $K_{\mathcal{D}}u_h \rightharpoonup \widehat{u}$ in $H^1(S, X^*), L^2(S, Y)$,

4. $K_{\mathcal{D}}u_h(t) \rightharpoonup \widehat{u}(t)$ in Y , and additionally in $L^p(\Omega)^m$ for $p \in [1, \infty)$ for all $t \in S$

as $\text{size}(\mathcal{D}) \rightarrow 0$. Note that, due to Theorem 3.5 we can extract a subsequence such that $K_{\mathcal{D}}u_h(t) \rightharpoonup \widehat{u}(t)$ in $L^p(\Omega)^m$ for $p \in [1, \infty)$ and for all $t \in S$. We also mention that due to Lemma A.3 we have $\bar{u}_h \rightarrow \bar{u}$ in Y . Moreover, by the definition of $K_{\mathcal{D}}$ and Lemma A.3 we have $u_h(0) = K_{\mathcal{D}}u_h(0) \rightarrow U$ in Y for $\text{size}(\mathcal{D}) \rightarrow 0$, hence $U = \widehat{u}(0)$. Using Definition 3.3 we find that

$$\begin{aligned} \|u_h - K_{\mathcal{D}}u_h\|_{L^2(S, X^*)}^2 &= \sum_{n=1}^N \int_{t_{n-1}}^{t_n} (t_n - t)^2 \|(K_{\mathcal{D}}u_h)'\|_{X^*}^2 dt \\ &\leq \bar{t}_\delta^2 \|(K_{\mathcal{D}}u_h)'\|_{L^2(S, X^*)}^2 \rightarrow 0 \end{aligned}$$

and therefore for subsequences $K_{\mathcal{D}}u_h(t) - u_h(t) \rightarrow 0$ in X^* and $u_h(t) \rightharpoonup \widehat{u}(t)$ in X^* f.a.a. $t \in S$ as $\text{size}(\mathcal{D}) \rightarrow 0$. Due to Lemma 4.1 and Theorem 3.5 we get $\sup_{\mathcal{D}} \|a_l(t)\|_Y < \infty$ for all $t \in S$, hence there exists a non-labeled subsequence, such that $a_l(t) \rightharpoonup \widehat{a}(t)$ in Y f.a.a. $t \in S$.

Strong convergence of the activities: Now we use a result of [23]: *Let $(\varphi_j)_{j \in \mathbb{N}}$ be an orthogonal basis of $L^2(\Omega)$. For all $\epsilon > 0$ there exists a $N_\epsilon > 0$ such that*

$$\|w\|_{L^2(\Omega)}^2 \leq \sum_{j=1}^{N_\epsilon} \langle w, \varphi_j \rangle_{L^2(\Omega)}^2 + \epsilon \|w\|_{H^1(\Omega)}^2 \quad \forall w \in H^1(\Omega). \quad (4.22)$$

We apply the result for different discretizations, i.e., $w = a_{\nu,l} - a_{\nu,l'}$, $\nu = 1, \dots, m$, and obtain after integration over S

$$\|a_{\nu,l} - a_{\nu,l'}\|_{L^2(S, L^2(\Omega))}^2 \leq \sum_{j=1}^{N_\epsilon} \int_0^T \langle a_{\nu,l} - a_{\nu,l'}, \varphi_j \rangle_{L^2(\Omega)}^2 dt + \epsilon \|a_{\nu,l} - a_{\nu,l'}\|_{L^2(S, H^1(\Omega))}^2.$$

Note the boundedness of $\sup_{\mathcal{D}} \|a_{\nu,l}\|_{L^2(S, H^1(\Omega))}$. Since $a_{\nu,l}$ is bounded in Y for all $t \in S$, by the dominated convergence theorem we conclude that $(a_{\nu,l})_{\mathcal{D}}$ is a Cauchy sequence in $L^2(S, L^2(\Omega))$ and therefore $a_{\nu,l} \rightarrow \widehat{a}_\nu$ in $L^2(S, L^2(\Omega))$ for $\nu = 1, \dots, m$. Since $u_h/\bar{u}_h = a_h$ and since $a_h - a_l \rightarrow 0$ in $L^2(S, Y)$ (see (1.31)) we obtain

$$\|u_h/\bar{u}_h - \widehat{a}\|_{L^2(S, Y)} \leq \|a_h - a_l\|_{L^2(S, Y)} + \|a_l - \widehat{a}\|_{L^2(S, Y)} \rightarrow 0.$$

On the other hand by using $u_h(t) \rightharpoonup \widehat{u}(t)$ in X^* f.a.a. $t \in S$ and $\sup_{\mathcal{D}} \|u_h(t)\|_Y < \infty$ for all $t \in S$ we obtain for a non-labeled subsequence $u_h(t) \rightharpoonup \widehat{u}(t)$ in Y f.a.a. $t \in S$. Now we apply the strong convergence of $\bar{u}_h \rightarrow \bar{u}$ in Y and the uniform boundedness from above and below of the sequence (\bar{u}_h) to get

$$u_h(t)/\bar{u}_h \rightharpoonup \widehat{u}(t)/\bar{u} \text{ in } Y \text{ f.a.a. } t \in S. \quad (4.23)$$

Finally, due to $\sup_{\mathcal{D}} \|u_h/\bar{u}_h\|_{L^2(S, Y)} < \infty$ we find by the dominated convergence theorem $u_h/\bar{u}_h \rightharpoonup \widehat{u}/\bar{u}$ in $L^2(S, Y)$ which gives us $\widehat{a} = \widehat{u}/\bar{u}$. Since a_h is uniformly bounded from above and below (see (3.16)) the bounds also hold for the limit \widehat{a} and therefore \widehat{a} is positive and $\widehat{v} := \ln \widehat{a}$.

From Lemma A.4 together with (A1) we conclude with some $c > 0$ that

$$\begin{aligned} \|R_{\nu h}(a_h) - R_{\nu}(\widehat{a})\|_{L^2(S, Y)}^2 &\leq c \|R_{\nu h}(a_h) - R_{\nu}(\widehat{a})\|_{L^1(S, Y)} \rightarrow 0, \\ \|\bar{u}_{\nu h} D_{\nu h}(a_h) - \bar{u}_{\nu} D_{\nu}(\widehat{a})\|_{L^2(S, Y)}^2 &\leq c \|\bar{u}_{\nu h} D_{\nu h}(a_h) - \bar{u}_{\nu} D_{\nu}(\widehat{a})\|_{L^1(S, Y)} \rightarrow 0 \end{aligned} \quad (4.24)$$

as $\text{size } \mathcal{D} \rightarrow 0$. This gives pointwise convergence a.e. for subsequences.

Weak solution: Since $C_0^\infty(\Omega)^m$ is dense in X we use test functions $\varphi \in C_0^\infty(\Omega)^m$ and a pure time function $\chi \in C_0^\infty(S)$. Set $\boldsymbol{\varphi} = (\varphi_\nu(x_K))_{K \in \mathcal{V}, \nu=1, \dots, m}$ and $\varphi_{\nu,h}(x) = \varphi_\nu(x_K)$ for $x \in K, K \in \mathcal{V}$. By $\varphi_{\nu,l}$ we denote the piecewise affine interpolation of $\boldsymbol{\varphi}$. Note that $\varphi_{\nu,l} \in L^\infty(\Omega)$. Let be $\bar{\chi}(t_n) = (\chi(t_n) + \chi(t_{n-1}))/2$ for $n = 1, \dots, N$. We note that

$$\begin{aligned} t_\delta^{(n)} \bar{\chi}(t_n) &= \frac{(t_\delta^{(n)})^2}{2t_\delta^{(n)}} (\chi(t_n) + \chi(t_{n-1})) \\ &= \frac{1}{t_\delta^{(n)}} \int_{t_{n-1}}^{t_n} \chi(t_n)(t - t_{n-1}) + \chi(t_{n-1})(t_n - t) dt \\ &= \int_{t_{n-1}}^{t_n} (K_{\mathcal{D}}\chi)(t) dt, \quad n = 1, \dots, N \end{aligned} \quad (4.25)$$

and $(K_{\mathcal{D}}\chi) \rightarrow \chi$ in $L^2(S)$ (use the mean-value form of the Taylor series remainder). We use test functions $\boldsymbol{\varphi} \bar{\chi}(t_n), t \in (t_{n-1}, t_n], n = 1, \dots, N$ for (3.11) and sum over $n = 1, \dots, N$ to obtain $S_1 + S_2 = S_3$ with

$$\begin{aligned} S_1 &:= \sum_{n=1}^N t_\delta^{(n)} \bar{\chi}(t_n) \left\langle \frac{\mathbf{u}(t_n) - \mathbf{u}(t_{n-1})}{t_\delta^{(n)}}, \boldsymbol{\varphi} \right\rangle_{\mathbb{R}^{Mm}}, \\ S_2 &:= \sum_{n=1}^N t_\delta^{(n)} \bar{\chi}(t_n) \sum_{\nu=1}^m \sum_{\sigma=T|L \in \mathcal{E}_{int}} T_\sigma Y_\nu^\sigma (a_{\nu L} - a_{\nu K}) (\varphi_{\nu L} - \varphi_{\nu K}), \\ S_3 &:= \sum_{n=1}^N t_\delta^{(n)} \bar{\chi}(t_n) \sum_{\nu=1}^m \sum_{K \in \mathcal{V}} |K| R_{\nu K}(\mathbf{a}_K) \varphi_{\nu K} \\ &= \sum_{\nu=1}^m \int_Q (K_{\mathcal{D}}\chi)(t) R_{\nu,h}(a_h) \varphi_{\nu,h} dx dt. \end{aligned}$$

We remark that the interpretation of the discrete sums as an integral over $Q = S \times \Omega$ like in the last two lines is crucial for the convergence proof. In the following we will do this several times. We define

$$\begin{aligned} \widehat{S}_1 &:= \int_S \langle \widehat{u}', \boldsymbol{\varphi} \rangle_X \chi dt, \\ \widehat{S}_2 &:= \sum_{\nu=1}^m \int_S \chi \int_\Omega D_\nu(\widehat{a}) \bar{u}_\nu \nabla \widehat{a}_\nu \cdot \nabla \varphi_\nu dt dx, \\ \widehat{S}_3 &:= \sum_{\nu=1}^m \int_S \chi \int_\Omega R_\nu(\widehat{a}) \varphi_\nu dx dt. \end{aligned}$$

Time derivative: Using (4.25) the term S_1 can be interpreted as

$$S_1 = \sum_{\nu=1}^m \int_Q \varphi_{\nu,h} ((K_{\mathcal{D}}u_{\nu,h})(t))' (K_{\mathcal{D}}\chi)(t) dx dt.$$

By partial time integration (and $K_{\mathcal{D}}\chi(0) = \chi(0) = \chi(t_N) = K_{\mathcal{D}}\chi(t_N) = 0$) we obtain

$$S_1 = - \sum_{\nu=1}^m \int_\Omega \int_S \varphi_{\nu,h} (K_{\mathcal{D}}u_{\nu,h})(t) ((K_{\mathcal{D}}\chi)(t))' dt dx.$$

Now we use $\varphi_h \rightarrow \varphi$ in Y , $(K_{\mathcal{D}}\chi)(t)' \rightarrow \chi'$ in $L^2(S)$, $K_{\mathcal{D}}u_h \rightarrow \widehat{u}$ in $L^2(S, Y)$ and $\widehat{u} \in H^1(S, X^*)$ to find

$$\lim_{\text{size } \mathcal{D} \rightarrow 0} S_1 = - \int_S \langle \widehat{u}, \boldsymbol{\varphi} \rangle_Y \chi' dt = \widehat{S}_1.$$

Reactions: Using (4.25) the reaction term S_3 can be written in the form $S_3 = S_{31} + S_{32}$,

$$S_{31} := \sum_{\nu=1}^m \int_S (K_{\mathcal{D}\chi})(t) \int_{\Omega} (R_{\nu,h}(a_h) - R_{\nu}(\hat{a})) \varphi_{\nu,h} dx dt,$$

$$S_{32} := \sum_{\nu=1}^m \int_S (K_{\mathcal{D}\chi})(t) \int_{\Omega} R_{\nu}(\hat{a}) \varphi_{\nu,h} dx dt.$$

Since $\varphi_h \rightarrow \varphi$ in Y we find $S_{32} \rightarrow \hat{S}_3$ and by Cauchy-Schwarz inequality we get

$$S_{31} \leq \sum_{\nu=1}^m \|(K_{\mathcal{D}\chi})(t) \varphi_{\nu,h}\|_{L^2(Q)} \|R_{\nu,h}(a_h) - R_{\nu}(\hat{a})\|_{L^2(Q)}.$$

For the first term we find $\lim_{\text{size } \mathcal{D} \rightarrow 0} \|(K_{\mathcal{D}\chi})(t) \varphi_{\nu,h}\|_{L^2(Q)} = \|\chi \varphi_{\nu}\|_{L^2(Q)}$ and due to (4.24) the second term tends to zero, and we find $\lim_{\text{size } \mathcal{D} \rightarrow 0} S_{31} = 0$, hence $\lim_{\text{size } \mathcal{D} \rightarrow 0} S_3 = \hat{S}_3$.

Diffusion: For the diffusion term we use (4.25) and the notation of Subsection 3.2 to get $S_2 = S_{21} + S_{22}$ with

$$S_{21} := \sum_{\nu=1}^m \int_S (K_{\mathcal{D}\chi})(t) \int_{\Omega} (D_{\nu,h}(a_h) \bar{u}_{\nu,h} - D_{\nu}(\hat{a}) \bar{u}_{\nu}) \nabla a_{\nu,l} \cdot \nabla \varphi_{\nu,l} dx dt,$$

$$S_{22} := \sum_{\nu=1}^m \int_S (K_{\mathcal{D}\chi})(t) \int_{\Omega} D_{\nu}(\hat{a}) \bar{u}_{\nu} \nabla a_{\nu,l} \cdot \nabla \varphi_{\nu,l} dx dt.$$

Applying Cauchy-Schwarz inequality and the boundedness of $K_{\mathcal{D}\chi} \nabla \varphi_{\nu,l}$ and of the reference densities we find with a constant $c > 0$

$$S_{21} \leq \sum_{\nu=1}^m c \|\nabla a_{\nu,l}\|_{L^2(S, L^2(\Omega)^2)} \|\bar{u}_{\nu,h} D_{\nu,h}(a_h) - \bar{u}_{\nu} D_{\nu}(\hat{a})\|_{L^2(S, L^2)},$$

and from (4.24) and Lemma 4.1 we obtain $S_{21} \rightarrow 0$ as $\text{size}(\mathcal{D}) \rightarrow 0$. For S_{22} we use weak-strong convergence with $a_l \rightharpoonup \hat{a}$ in $L^2(S, X)$ and $(K_{\mathcal{D}\chi}) \varphi_l \rightarrow \chi \varphi$ in $L^2(S, X)$ to find $\lim_{\text{size } \mathcal{D} \rightarrow 0} S_{22} = \hat{S}_2$ hence $\lim_{\text{size } \mathcal{D} \rightarrow 0} S_2 = \hat{S}_2$. Since $S_1 + S_2 = S_3$ and $\lim_{\text{size } \mathcal{D} \rightarrow 0} S_i = \hat{S}_i$ for $i = 1, 2, 3$ we have shown that $(\hat{u}, \hat{v}) = (\hat{u}, \ln \hat{a})$ is a weak solution of the continuous problem (P) in the sense of (2.6).

Strong convergence of the gradient: Now we prove the strong convergence of the gradient. Since we know that $(\hat{u}, \hat{v}) = (\hat{u}, \ln \hat{a})$ is a weak solution of the continuous problem (P) and by testing (P) with $\hat{a} \in L^2(S, X)$ we find $\hat{S}_1 + \hat{S}_2 = \hat{S}_3$ with

$$\hat{S}_1 := \int_S \langle \hat{u}', \hat{a} \rangle_X dt = \hat{S}_{11} - \hat{S}_{12},$$

$$\hat{S}_{11} := \sum_{\nu=1}^m \int_{\Omega} \frac{\hat{u}_{\nu}^2(t_N)}{2\bar{u}_{\nu}} dx, \quad \hat{S}_{12} := \sum_{\nu=1}^m \int_{\Omega} \frac{U_{\nu}^2}{2\bar{u}_{\nu}} dx,$$

$$\hat{S}_2 := \sum_{\nu=1}^m \int_Q D_{\nu} \bar{u}_{\nu} |\nabla \hat{a}_{\nu}|^2 dt dx, \quad \hat{S}_3 := \sum_{\nu=1}^m \int_Q R_{\nu}(\hat{a}) \hat{a}_{\nu} dt dx.$$

Testing the discrete problem $(P_{\mathcal{D}})$ with the discrete vector $\mathbf{a} \in \mathbb{R}^{Mm}$ (defining the quantities a_h and a_l) we find analogously to the continuous problem $S_1 + S_2 = S_3$ with

$$S_1 := \sum_{\nu=1}^m \int_Q (K_{\mathcal{D}} u_{\nu,h}(t))' a_{\nu,h}(t) dx dt, \quad S_2 := \sum_{\nu=1}^m \int_Q D_{\nu,h}(a_h) \bar{u}_{\nu,h} |\nabla a_{\nu,l}|^2 dx dt,$$

$$S_3 := \sum_{\nu=1}^m \int_Q R_{\nu,h}(a_h) a_{\nu,h} dx dt.$$

Time derivative: Using $(x - y)x \geq \frac{1}{2}(x^2 - y^2) \forall x, y \in \mathbb{R}$ we estimate

$$\begin{aligned}
S_1 &= \sum_{\nu=1}^m \sum_{n=1}^N \int_{t_{n-1}}^{t_n} \int_{\Omega} \left(\frac{u_{\nu,h}(t_n) - u_{\nu,h}(t_{n-1})}{t_n - t_{n-1}} \right) a_{\nu,h}(t_n) dx dt \\
&\geq \sum_{\nu=1}^m \sum_{n=1}^N \int_{t_{n-1}}^{t_n} \int_{\Omega} \frac{1}{2\bar{u}_{\nu,h}} \left(\frac{u_{\nu,h}^2(t_n) - u_{\nu,h}^2(t_{n-1})}{t_n - t_{n-1}} \right) dx dt \\
&= \sum_{\nu=1}^m \int_Q \frac{\left(K_{\mathcal{D}} u_{\nu,h}^2(t) \right)'}{2\bar{u}_{\nu,h}} dx dt \\
&= S_{11} - S_{12},
\end{aligned}$$

where

$$S_{11} := \sum_{\nu=1}^m \int_{\Omega} \frac{u_{\nu,h}^2(t_N)}{2\bar{u}_{\nu,h}} dx, \quad S_{12} := \sum_{\nu=1}^m \int_{\Omega} \frac{u_{\nu,h}^2(0)}{2\bar{u}_{\nu,h}} dx.$$

Using weak strong convergence for $u_h(0) = (K_{\mathcal{D}} u_h)(0) \rightharpoonup \hat{u}(0)$ and also for $u_h(t_N) = (K_{\mathcal{D}} u_h)(t_N) \rightharpoonup \hat{u}(t_N)$ in $L^4(\Omega)^m$ together with $1/\bar{u}_h \rightarrow 1/\bar{u}$ in Y we get $S_{12} \rightarrow \hat{S}_{12}$ and $S_{11} \rightarrow \hat{S}_{11}$ as $\text{size}(\mathcal{D}) \rightarrow 0$.

Reactions: By Cauchy-Schwarz inequality we obtain for the reaction term $S_3 = S_{31} + S_{32}$,

$$\begin{aligned}
S_{31} &:= \sum_{\nu=1}^m \int_Q a_{\nu,h} (R_{\nu,h}(a_h) - R_{\nu}(\hat{a})) dx dt \\
&\leq \sum_{\nu=1}^m \|a_{\nu,h}\|_{L^2(S,L^2)} \|R_{\nu,h}(a_h) - R_{\nu}(\hat{a})\|_{L^2(S,L^2)}, \\
S_{32} &:= \sum_{\nu=1}^m \int_Q R_{\nu}(\hat{a}) a_{\nu,h} dx dt.
\end{aligned}$$

Due to (4.24) and Theorem 3.5 we find $S_{31} \rightarrow 0$ and by $a_h \rightarrow \hat{a}$ in $L^2(S, Y)$ we obtain $S_{32} \rightarrow \hat{S}_3$, hence $S_3 \rightarrow \hat{S}_3$ as $\text{size}(\mathcal{D}) \rightarrow 0$.

Diffusion: By $S_{11} - S_{12} \leq S_1 = -S_2 + S_3$ leading to $S_{11} + S_2 \leq S_3 + S_{12}$ we find

$$\hat{S}_{11} + \limsup_{\text{size } \mathcal{D} \rightarrow 0} S_2 = \limsup_{\text{size } \mathcal{D} \rightarrow 0} (S_{11} + S_2) \leq \limsup_{\text{size } \mathcal{D} \rightarrow 0} (S_3 + S_{12}) = \hat{S}_3 + \hat{S}_{12}$$

and by $\hat{S}_3 = \hat{S}_{11} - \hat{S}_{12} + \hat{S}_2$ we obtain

$$\limsup_{\text{size } \mathcal{D} \rightarrow 0} S_2 \leq \hat{S}_2. \tag{4.26}$$

Exploiting (4.24) and using $D_{\nu,h} \bar{u}_{\nu,h} \rightarrow D_{\nu} \bar{u}_{\nu}$ for a.a. $(x, t) \in Q$ and the boundedness of the diffusion coefficients and the reference densities (see (A1)) we find $\sqrt{D_{\nu,h} \bar{u}_{\nu,h}} \varphi_{\nu} \rightarrow \sqrt{D_{\nu} \bar{u}_{\nu}} \varphi_{\nu}$ in $L^2(Q)$ for all $\varphi \in L^2(S, Y)$ and $\sqrt{D_{\nu,h} \bar{u}_{\nu,h}} \rightarrow \sqrt{D_{\nu} \bar{u}_{\nu}}$ for a.a. $(x, t) \in Q$. Therefore using $\nabla a_l \rightharpoonup \nabla \hat{a}$ in $L^2(S, Y^2)$ we obtain

$$\begin{aligned}
&\sum_{\nu=1}^m \int_Q \left(\sqrt{D_{\nu,h} \bar{u}_{\nu,h}} \nabla a_{\nu,l} - \sqrt{D_{\nu} \bar{u}_{\nu}} \nabla \hat{a}_{\nu} \right) \varphi_{\nu} dx dt \\
&= \sum_{\nu=1}^m \int_Q \sqrt{D_{\nu,h} \bar{u}_{\nu,h}} (\nabla a_{\nu,l} - \nabla \hat{a}_{\nu}) \varphi_{\nu} dx dt \\
&+ \sum_{\nu=1}^m \int_Q \left(\sqrt{D_{\nu,h} \bar{u}_{\nu,h}} - \sqrt{D_{\nu} \bar{u}_{\nu}} \right) \nabla \hat{a}_{\nu} \varphi_{\nu} dx dt \rightarrow 0
\end{aligned}$$

for all $\varphi \in L^2(S, Y)$ as $\text{size}(\mathcal{D}) \rightarrow 0$. This weak convergence gives us

$$\liminf_{\text{size } \mathcal{D} \rightarrow 0} S_2 = \liminf_{\text{size } \mathcal{D} \rightarrow 0} \sum_{\nu=1}^m \left\| \sqrt{D_{\nu,h} \bar{u}_{\nu,h}} \nabla a_{\nu,l} \right\|_{L^2(Q)}^2 \geq \sum_{\nu=1}^m \left\| \sqrt{D_{\nu} \bar{u}_{\nu}} \nabla \hat{a}_{\nu} \right\|_{L^2(Q)}^2 = \hat{S}_2.$$

Together with (4.26) it follows

$$\lim_{\text{size } \mathcal{D} \rightarrow 0} S_2 = \hat{S}_2. \quad (4.27)$$

Now we prove $\|a_l - \hat{a}\|_{L^2(S, X)} \rightarrow 0$ as $\text{size}(\mathcal{D}) \rightarrow 0$. Using (A1) we calculate with some constant $c > 0$

$$\begin{aligned} \|\nabla a_l - \nabla \hat{a}\|_{L^2(S, Y^2)}^2 &= \sum_{\nu=1}^m \int_Q \frac{D_{\nu,h}(a_h) \bar{u}_{\nu,h}}{D_{\nu,h}(a_h) \bar{u}_{\nu,h}} |\nabla a_{\nu,l} - \nabla \hat{a}_{\nu}|^2 dx dt \\ &\leq c \sum_{\nu=1}^m \int_Q D_{\nu,h}(a_h) \bar{u}_{\nu,h} |\nabla a_{\nu,l} - \nabla \hat{a}_{\nu}|^2 dx dt \\ &= c(S_{21} - 2S_{22} + S_{23}) \end{aligned}$$

with

$$\begin{aligned} S_{21} &:= \sum_{\nu=1}^m \int_Q D_{\nu,h}(a_h) \bar{u}_{\nu,h} |\nabla a_{\nu,l}|^2 dx dt \\ S_{22} &:= \sum_{\nu=1}^m \int_Q D_{\nu,h}(a_h) \bar{u}_{\nu,h} \nabla a_{\nu,l} \cdot \nabla \hat{a}_{\nu} dx dt \\ S_{23} &:= \sum_{\nu=1}^m \int_Q D_{\nu,h}(a_h) \bar{u}_{\nu,h} |\nabla \hat{a}_{\nu}|^2 dx dt. \end{aligned}$$

Using Cauchy-Schwarz inequality we find $S_{22} = S_{221} + S_{222}$ with

$$\begin{aligned} S_{221} &:= \sum_{\nu=1}^m \int_Q (D_{\nu,h}(a_h) \bar{u}_{\nu,h} - D_{\nu}(\hat{a}) \bar{u}_{\nu}) \nabla a_{\nu,l} \cdot \nabla \hat{a}_{\nu} dx dt \\ &\leq \|a_l\|_{L^2(S, X)} \sum_{\nu=1}^m \|(D_{\nu,h}(a_h) \bar{u}_{\nu,h} - D_{\nu}(\hat{a}) \bar{u}_{\nu}) \nabla \hat{a}_{\nu}\|_{L^2(S, L^2)}, \\ S_{222} &:= \sum_{\nu=1}^m \int_Q D_{\nu}(\hat{a}) \bar{u}_{\nu} \nabla \hat{a}_{\nu} \cdot \nabla a_{\nu,l} dx dt. \end{aligned}$$

By (4.24) we obtain the pointwise convergence of $D_{\nu,h}(a_h) \bar{u}_{\nu,h} \rightarrow D_{\nu}(\hat{a}) \bar{u}_{\nu}$ and by dominated convergence theorem we find $S_{221} \rightarrow 0$ and $S_{23} \rightarrow \hat{S}_2$ as $\text{size}(\mathcal{D}) \rightarrow 0$. By the weak convergence of $a_l \rightharpoonup \hat{a}$ in $L^2(S, X)$ we get $S_{222} \rightarrow \hat{S}_2$, hence $S_{22} \rightarrow \hat{S}_2$. From (4.27) we have $S_{21} \rightarrow \hat{S}_2$ and therefore $S_{21} - 2S_{22} + S_{23} \rightarrow 0$ as $\text{size}(\mathcal{D}) \rightarrow 0$. \square

Corollary 4.3. *Let (A1) be fulfilled and let $\mathcal{D} = (\mathcal{M}, (t_{\delta}^n)_{n=1}^N)$ be a sequence of discretizations fulfilling (A2). Moreover, let (\hat{u}, \hat{v}) be a weak solution of the continuous problem (P). Then there exists a subsequence of solutions (u_h, v_h) to $(P_{\mathcal{D}})$ with the convergence properties stated in Theorem 4.2 such that*

$$\|F_h(u_h) - F(\hat{u})\|_{L^2(S)} \rightarrow 0 \text{ as } \text{size}(\mathcal{D}) \rightarrow 0.$$

Moreover, for the relative free energy $\Psi_h(u_h) := F_h(u_h) - F_h(u_h^*)$ holds

$$\|\Psi_h(u_h) - \Psi(\hat{u})\|_{L^2(S)} \rightarrow 0 \text{ as } \text{size}(\mathcal{D}) \rightarrow 0. \quad (4.28)$$

Proof. Let c be a positive constant with varying meaning. Thanks to Theorem 3.5 we get

$$\begin{aligned} \|\ln(u_h/\bar{u}_h) - \ln(\hat{u}/\bar{u})\|_{L^2(S,Y)} &= \|\ln a_h - \ln \hat{a}\|_{L^2(S,Y)} \\ &\leq \frac{\|a_h - \hat{a}\|_{L^2(S,Y)}}{\min_{\nu=1,\dots,m} \operatorname{ess\,inf}_{x \in \Omega} \hat{a}_\nu(x)} \rightarrow 0 \end{aligned}$$

and together with Lemma A.3 and $u_h \rightarrow \hat{u}$ in $L^2(S, Y)$ we obtain the following estimate

$$\begin{aligned} S_1 &= \|F_h(u_h) - F(\hat{u})\|_{L^2(S)}^2 \\ &\leq c \|\ln(u_h/\bar{u}_h) - \ln(\hat{u}/\bar{u})\|_{L^2(S,Y)}^2 + c \|u_h - \hat{u}\|_{L^2(S,Y)}^2 + c T \|\bar{u}_h - \bar{u}\|_Y^2 \rightarrow 0, \end{aligned}$$

as $\operatorname{size}(\mathcal{D}) \rightarrow 0$.

Since $u_h^* = \frac{\bar{u}_h}{\bar{u}} u^*$ and $a_h^* = a^*$ holds (see [15, Corollary 3.1]) and by Lemma A.3, we find

$$\|F_h(u_h^*) - F(u^*)\|_{L^2(S)}^2 \leq c T \sum_{\nu=1}^m \|a_\nu^* (\ln a_\nu^* - 1) + 1\|_{L^\infty(\Omega)} \|\bar{u}_{\nu,h} - \bar{u}_\nu\|_{L^2(\Omega)}^2 \rightarrow 0,$$

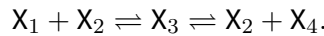
from which the second assertion follows. \square

Remark 4.4. In the case where, the diffusion coefficients only depend on the space variable and not on the state variable we have uniqueness of the weak solution (\hat{u}, \hat{v}) of the continuous problem (P) as proven in [19, Theorem 5.6]. Assume by contradiction that there exist two converging subsequences, then one can repeat the proof of Theorem 3.6 and Section 4 and use [19, Theorem 5.6] to conclude that there exists only one limit point. Therefore not only a subsequence converges, but so does the whole sequence.

5. Numerical example

We close the paper by a numerical simulation of the *Michaelis-Menten-Henri mechanism* (MMH), from an initial value until thermodynamic equilibrium. This reaction system is well-known in biology and chemistry, see [22, 25, 31]. For an example occurring in the simulation of the post-exposure-bake step in optical lithography we refer to [24, 9, 10].

The MMH-mechanism is the reaction system



Here an enzyme X_1 reacts with the substrate X_2 to form a complex X_3 which then decays to the product X_4 and releases the substrate X_2 . Correspondingly, the set \mathcal{R} consists of two pairs of vectors, namely $\alpha_1 = (1, 1, 0, 0)$ and $\beta_1 = (0, 0, 1, 0)$ for the first reaction as well as $\alpha_2 = (0, 0, 1, 0)$ and $\beta_2 = (0, 1, 0, 1)$ for the second reaction.

Due to the definition of the reaction term (1.3), the net production rates of the species are given by

$$\begin{aligned} R_1(a) &= -k_{(\alpha_1, \beta_1)}(a_1 a_2 - a_3), \\ R_2(a) &= -k_{(\alpha_1, \beta_1)}(a_1 a_2 - a_3) && + k_{(\alpha_2, \beta_2)}(a_3 - a_2 a_4), \\ R_3(a) &= +k_{(\alpha_1, \beta_1)}(a_1 a_2 - a_3) && - k_{(\alpha_2, \beta_2)}(a_3 - a_2 a_4), \\ R_4(a) &= && + k_{(\alpha_2, \beta_2)}(a_3 - a_2 a_4). \end{aligned}$$

The stoichiometric subspace \mathcal{S} and its orthogonal complement \mathcal{S}^\perp are spanned by

$$\mathcal{S} = \operatorname{span}\{(1, 1, -1, 0), (0, -1, 1, -1)\}, \quad \mathcal{S}^\perp = \operatorname{span}\{(1, 0, 1, 1), (0, 1, 1, 0)\}.$$

Every element of \mathcal{S}^\perp creates one invariant of the system, i.e., $R_1 + R_3 + R_4 \equiv 0$ and $R_2 + R_3 \equiv 0$ hold, and hence

$$\int_{\Omega} (u_1 + u_3 + u_4)(t) dx = \int_{\Omega} (U_1 + U_3 + U_4) dx, \quad (5.29)$$

$$\int_{\Omega} (u_2 + u_3)(t) dx = \int_{\Omega} (U_2 + U_3) dx \quad \forall t \geq 0 \quad (5.30)$$

are conserved during the time evolution (use the homogeneous Neumann boundary conditions and integration over the entire domain). At thermodynamic equilibrium the chemical activities are constant over all control volumes $K \in \mathcal{V}$, therefore the solution can be obtained by solving

$$0 = R_1(a^*) = a_1^* a_2^* - a_3^*, \quad 0 = R_4(a^*) = a_2^* a_4^* - a_3^*$$

together with (5.29), (5.30). In the model that we have in mind [10, 9], the diffusion coefficient of X_2 is given by

$$D_2(a_1, a_4) = D_{20} \exp \left(-\varphi_3 \frac{\varphi_1 \bar{u}_1 a_1 + (1 - \varphi_1) \bar{u}_4 a_4}{\varphi_2 \bar{u}_1 a_1 + (1 - \varphi_2) \bar{u}_4 a_4} \right),$$

where $\varphi_1, \varphi_2, \varphi_3$ are so-called lumped constants, see [10]. All other diffusion coefficients are assumed to be piecewise constant and independent of the concentration.

Time integration is done using the fully implicit Euler discretization, where the initial guess of the Newton iteration is predicted by a linear extrapolation in time of the last two previous accepted solutions for the chemical potentials.

The time step of the method is adapted to the variation of the free energy, the dissipation rate of the system, and the number of necessary iterations for Newton's method. If possible, the time step is incremented by a fixed constant (in the simulations by 1.6).

The nonlinear systems are solved by Newton's method and the resulting linear systems are solved by the sparse direct solver PARDISO [29, 30]. Due to roundoff errors the invariants can be driven away during the time evolution. The same behavior is known in the context of solving numerically ODEs with linear constraints, see [4]. Therefore we introduce two Lagrange multipliers to stay on the manifold spanned by (5.29)-(5.30). The Newton iteration stops if $\|\delta_v\|_{L^\infty} \leq \epsilon_r$ where δ_v is the Newton update of chemical potentials and ϵ_r is a given tolerance [13] and if the relative mass invariant error is less than a given tolerance.

We are interested in the behavior of the method using different discretizations for $Q = S \times \Omega$, i.e., using different meshes and different adaptive time-steppings. For $\Omega \subset \mathbb{R}^2$, we choose a circular domain consisting of three different materials, see Figure 3. The material boundaries are aligned to the edges of the triangles and every subdomain fulfills the boundary conforming Delaunay property. The Delaunay meshes are created by TRIANGLE [32] and have a different number of nodes, see Table 1. In the fourth column, we compute the ratio of mesh $\mathcal{M}_i, i = 1 \dots, 4$, related to \mathcal{M}_5 . The materials are represented by

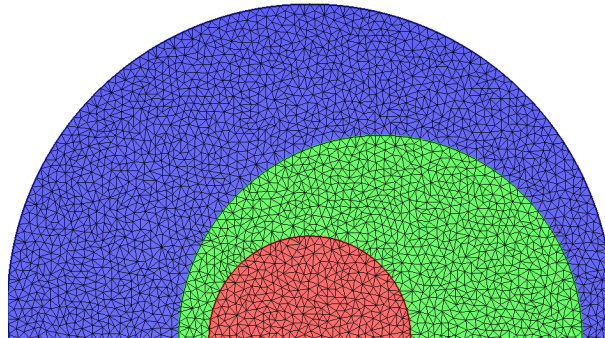


Figure 3: Mesh \mathcal{M}_2 : One half of the grid is shown. The different colors represent different materials

Mesh	$\#\mathcal{P}$	$\#\mathcal{T}$	ratio
\mathcal{M}_1	465	861	0.01
\mathcal{M}_2	2264	4360	0.05
\mathcal{M}_3	4454	8687	0.1
\mathcal{M}_4	22085	43666	0.5
\mathcal{M}_5	43973	87233	1

Table 1: Characterization of the different meshes

	red region	green region	blue region
(\bar{u}_1, \bar{u}_2)	$(10^{-16}, 10)$	$(1, 1)$	$(10^{-20}, 1)$
(\bar{u}_3, \bar{u}_4)	$(10, 10^{12})$	$(1, 1)$	$(10^{-11}, 1)$
(U_1, U_2)	$(1, 10^{-15})$	$(1, 1)$	$(10^{-20}, 10^{-16})$
(U_3, U_4)	$(10^{-15}, 10^{-16})$	$(1, 1)$	$(1, 10^{-27})$
(D_1, D_{20})	$(10^{-10}, 200)$	$(10^{-10}, 0.02)$	$(10^{-10}, 250)$
(D_3, D_4)	$(10^{-10}, 10^{-12})$	$(10^{-5}, 10^{-12})$	$(10^{-10}, 10^{-12})$
$(\varphi_3, \varphi_1, \varphi_2)$	$(3.37, 0.65, 0.95)$	$(10, 0.01, 0.95)$	$(0, 0.65, 0.95)$
$(k_{(\alpha_1, \beta_1)}, k_{(\alpha_2, \beta_2)})$	$(10^{-9}, 10^3)$	$(10^{+10}, 10)$	$(10^{-21}, 0.1)$

Table 2: Material parameter for the three different regions. Note the large differences in the diffusion and reaction coefficients

different colors in the mesh and the used parameters are collected in Table 2. The simulation parameters in the blue region are chosen in such a way that the catalyst X_2 is created by the intermediate X_3 . In the red region the forward direction of the MMH mechanism dominates. We expect that the catalyst X_2 from the green region diffuses and creates together with X_1 the intermediate X_3 which quickly degrades into X_4 by releasing X_2 . On the slow timescales the created structures dissolve by diffusion and the thermodynamic equilibrium solution is attained. The parameters in the green region are chosen in such a way that the reaction is in steady state. Due to changes in the blue region the steady state is violated and the reaction and diffusion processes start.

At thermodynamic equilibrium, the chemical activities are given in Table 3. Since we are interested

Mesh	$a_{1,h}^*$	$a_{2,h}^*$	$a_{3,h}^*$	$a_{4,h}^*$
\mathcal{M}_1	$1.626 \cdot 10^{-11}$	0.643	$1.044 \cdot 10^{-11}$	$1.626 \cdot 10^{-11}$
\mathcal{M}_2	$1.549 \cdot 10^{-11}$	0.624	$9.670 \cdot 10^{-12}$	$1.549 \cdot 10^{-11}$
\mathcal{M}_3	$1.534 \cdot 10^{-11}$	0.620	$9.517 \cdot 10^{-12}$	$1.534 \cdot 10^{-11}$
\mathcal{M}_4	$1.515 \cdot 10^{-11}$	0.615	$9.319 \cdot 10^{-12}$	$1.515 \cdot 10^{-11}$
\mathcal{M}_5	$1.510 \cdot 10^{-11}$	0.614	$9.273 \cdot 10^{-12}$	$1.510 \cdot 10^{-11}$

Table 3: Thermodynamic equilibrium of the system on different meshes. Note that the equilibrium solution is constant for all $K \in \mathcal{V}$. Moreover, it depends slightly on the geometric approximation of the curved boundaries of the domain by the triangulations

in the long time behavior of the method, we run the simulation on a time interval $S = [0, 10^{20}]$. The number of executed (excluding rejections) time steps, the number of rejections, and the squared ratio of used time steps related to discretization \mathcal{D}_5 are tabulated in Table 4. In addition, the $L^2(S)$ -norm of the relative free energy functional and the dissipation rate are summarized. The ratio of the mesh nodes and the squared ratio of the executed time steps are close together. In Figure 4, we plot the increase of the time step over the time. The time step grows linearly in the log-log scale, except when a new time scale is reached. The first deviation from linear growth in log-log-scale is due to the fast reaction in the blue

Discret.	# times.;rej	ratio sq	$\ \Psi_{h_i}\ _{L^2(S)}$	$\ D_{h_i}\ _{L^2(S)}$
\mathcal{D}_1	834; 4	0.027	$1.835 \cdot 10^8$	$3.082 \cdot 10^7$
\mathcal{D}_2	1104; 5	0.047	$1.886 \cdot 10^8$	$3.294 \cdot 10^7$
\mathcal{D}_3	1693; 4	0.11	$1.890 \cdot 10^8$	$3.339 \cdot 10^7$
\mathcal{D}_4	3513; 3	0.48	$1.893 \cdot 10^8$	$3.397 \cdot 10^7$
\mathcal{D}_5	5084; 3	1	$1.894 \cdot 10^8$	$3.414 \cdot 10^7$

Table 4: Characterization of the time discretizations: Shown are the total number of time steps (without rejections) that are needed by the program in order to solve the problem on $S = [0, 10^{20}]$, the squared ratio of the necessary time steps w.r.t. the finest discretization \mathcal{D}_5 , and the $L^2(S)$ -norm of the relative free energy and the dissipation rate

region. During the movement of the front of X_4 , the time step is limited by the number of Newton steps. The second deviation is less pronounced on the coarse mesh, due to a faster discrete diffusion on coarse meshes. The next deviation is due to the growth of the concentration on the boundary between the green and red region. The finer mesh resolves more effects of the solution, therefore the necessary time steps for \mathcal{D}_5 are smaller compared to the time steps of \mathcal{D}_1 .

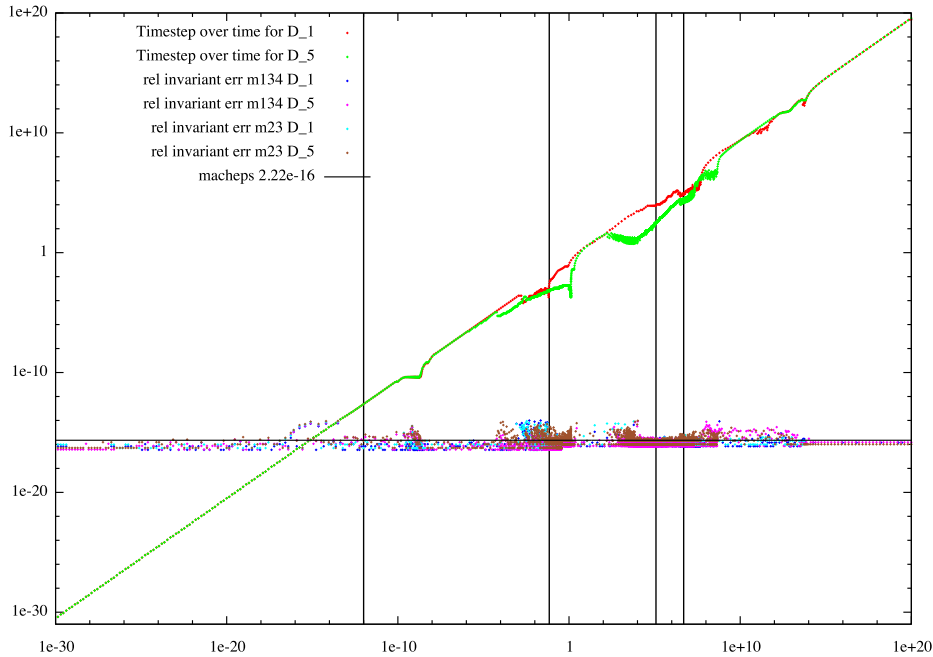


Figure 4: Evolution of the time step over the time for the discretizations \mathcal{D}_1 and \mathcal{D}_5 . Relative error of the conservation of invariants (5.29) and (5.30) during time evolution

Since the problem is nonlinear and an analytical solution is only available at thermodynamic equilibrium we study the convergence of the method by exploiting the difference of the relative free energy, and the reaction and diffusion part of the dissipation rate, see Corollary 4.3. In a first step the system forms X_2 in the blue region. Due to the strongly spatially varying diffusivity of X_4 the concentration creates a wall on the boundary of two materials. Then the movement of X_4 into the red region starts. On the coarsest mesh the diffusion is larger, therefore the front moves faster and the dissipation rate disappears earlier in time. After the species X_4 fully fills up the red region, the wall on the boundary of the red and green region starts to grow. The growth is driven by reaction and diffusion and will become flatter on the area where the distance of the red and blue region is minimal. The species X_4 can not penetrate into the red

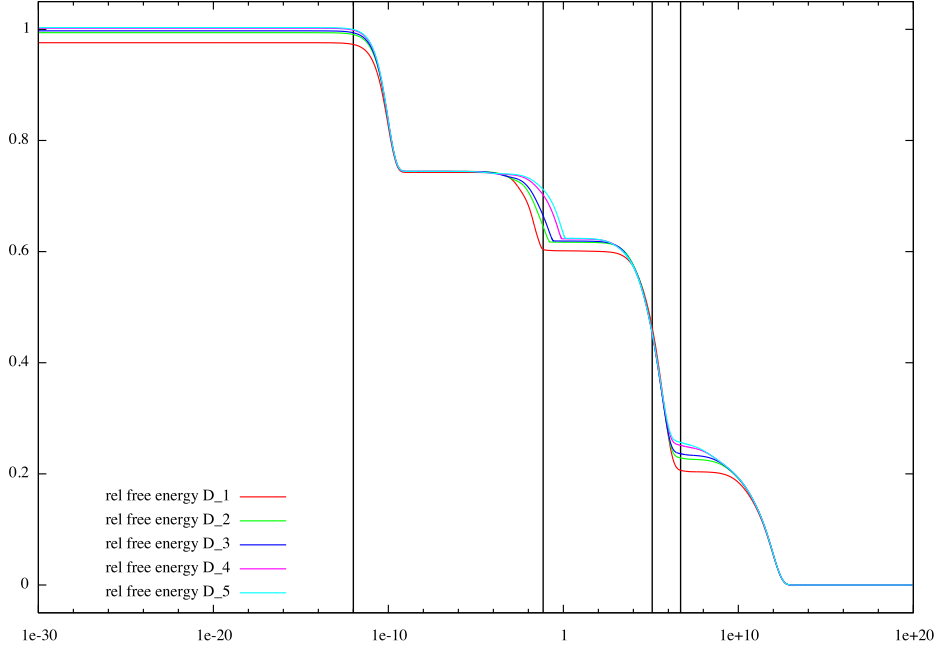


Figure 5: Evolution of the relative free energy functional Ψ_{h_i} for different discretizations \mathcal{D}_i , $i = 1, \dots, 5$. The function values are scaled by 1720

region due to its very small diffusivity. After the system is evolving on the slow time scale, the barrier dissolves and the concentration of species X_4 raises in the red region and the system approximates the thermodynamic equilibrium. In Figure 6 we depict the evolution of concentration of the for species on the mesh \mathcal{M}_1 and \mathcal{M}_5 at various times. Every column in Figure 6 corresponds to a vertical straight line in the relative free energy plots in Figure 5.

The evolution of the relative free energy functional Ψ_h is plotted in Figure 5. The evolution of the relative free energy and the dissipation rate reflects the different timescales of the system. Since the initial value is differently resolved by the meshes, the relative free energy varies on different meshes at the initial time. After the first fast reaction the curve of the relative free energy steps down. Since the reaction is faster than all other diffusion timescales the curves nearly coincide. Coarse grids add numeric diffusion, hence the front movement is slower on fine grids and the energy curves decay accordingly. Then further diffusion is blocked by the already described wall and this causes the synchronization of all free energy curves. The fill up of the red region by X_4 is diffusion dominated and depends on the refinement of the mesh. Therefore we see a time shift in the free energy curves. Finally the system approximates the thermodynamic equilibrium, which depends on the initial species masses, hence weakly on the spatial discretization. This is reflected in nearly coinciding energy curves.

In Figure 7 we plot the evolution of the absolute difference of the free energy curve associated to \mathcal{D}_i , $i = 1, \dots, 4$, and the free energy curve belonging to \mathcal{D}_5 . In Table 5 the relative $L^2(S)$ -error of the relative free energy and the dissipation rate is presented. Since the continuous solution of the reaction-diffusion system is not known, a reference solution for the finest discretization \mathcal{D}_5 is computed, and errors are measured against this discrete solution. From these errors convergence rates are estimated by fitting. We investigate only the convergence behavior w.r.t. the spatial error, since in our scheme the time step adaptation is intimately coupled to the space discretization. The error norms are given by

$$\begin{aligned} \left\| \tilde{\Psi}_{h_{ij}} \right\|_{L^2(S)} &= \left\| \Psi_{h_i}(u_{h_i}) - \Psi_{h_j}(u_{h_j}) \right\|_{L^2(S)} \left\| \Psi_{h_j}(u_{h_j}) \right\|_{L^2(S)}^{-1}, \\ \left\| \tilde{D}_{h_{ij}} \right\|_{L^2(S)} &= \left\| D_{h_i}(u_{h_i}) - D_{h_j}(u_{h_j}) \right\|_{L^2(S)} \left\| D_{h_j}(u_{h_j}) \right\|_{L^2(S)}^{-1}. \end{aligned}$$

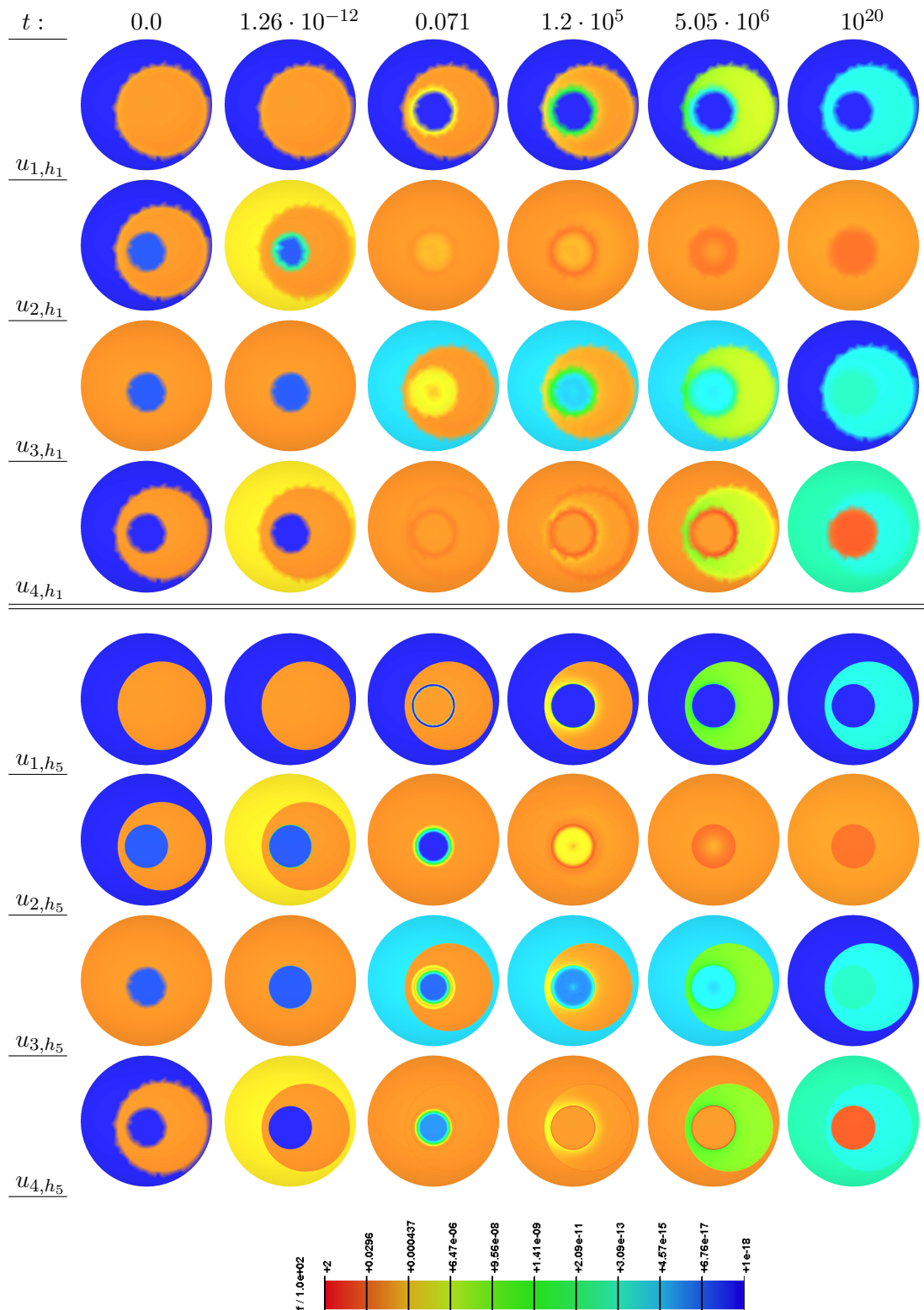


Figure 6: Concentrations of the four species at different times for discretizations \mathcal{D}_1 and \mathcal{D}_5 . Note the similarities of the coarse and fine solutions, e.g., at $t = 1.26 \cdot 10^{-12}$ and $t = 5.05 \cdot 10^6$. Be aware that differences are mainly caused by faster diffusion on coarse grids

For the estimate of the convergence order, only the results from the first three discretizations \mathcal{D}_1 , \mathcal{D}_2 and \mathcal{D}_3 are taken into account. The results from discretization \mathcal{D}_4 are too close to the results of discretization

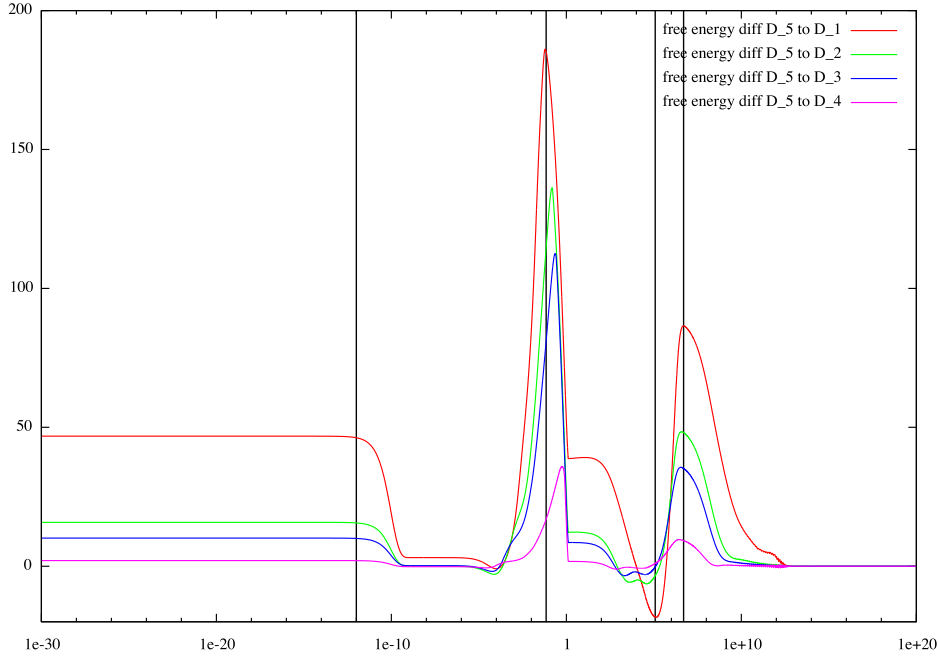


Figure 7: Evolution of the difference of the relative free energy functional Ψ_{h_i} of the discretization \mathcal{D}_i , $i = 1, \dots, 4$, relative to the relative free energy curve of discretization \mathcal{D}_5

\mathcal{D}_5 , and therefore higher-order components of the true error can spoil the error $\|\tilde{\Psi}_{h_{i5}}\|_{L^2(S)}$. This is a typical phenomenon, when an error norm is computed against a fine-grid reference solution, and not the true reference solution. Defining $h = \frac{1}{\sqrt{\#\mathcal{P}}}$, one can recognize from Table 5 that the $L^2(S)$ -errors of the relative free energy and the dissipation rate decay as h^2 and $h^{1.3}$. Note that the used number of time steps is proportional to $\frac{1}{h}$, as can be seen from the ratios of Table 1 and 4. Therefore, we observe that our scheme allows by doubling the number of time steps and quadrupling the number of mesh points to divide the error of the discrete relative free energy by a factor of four.

	$\#\mathcal{P}$	$\#\text{time step}$	$\ \tilde{\Psi}_{h_{i5}}\ _{L^2(S)}$	$\ \tilde{D}_{h_{i5}}\ _{L^2(S)}$
\mathcal{D}_1	465	834	$3.222 \cdot 10^{-2}$	$9.7169 \cdot 10^{-2}$
\mathcal{D}_2	2264	1104	$5.551 \cdot 10^{-3}$	$3.5055 \cdot 10^{-2}$
\mathcal{D}_3	4454	1693	$3.171 \cdot 10^{-3}$	$2.2047 \cdot 10^{-2}$
\mathcal{D}_4	22085	3513	$4.561 \cdot 10^{-3}$	$4.8920 \cdot 10^{-3}$

Table 5: $L^2(S)$ -norm of the relative free energy Ψ_{h_i} and the dissipation rate D_{h_i} of discretization \mathcal{D}_i , $i = 1, \dots, 4$, related to discretization \mathcal{D}_5 and scaled by the $L^2(S)$ -norm of the relative free energy and dissipation rate of \mathcal{D}_5

We emphasize that our method can approximate the thermodynamic equilibrium and it shows the expected decay of the relative free energy and the expected nonnegativity of the dissipation rate on all considered discretizations. All timescales of the system can be resolved by the method, even if the front movement or the strong gradients in the direct neighborhood of interfaces are only roughly resolved — still on the very coarse mesh \mathcal{M}_1 the different energetic states of the system are present, of course with time shifts of their begin and end points (compare Figures 5, 6, 7). In general, diffusion is faster on coarse grids due to the added numerical diffusion. Whenever a quasi steady state at a time scale is reached, or the system is 'waiting' before evolving on the next slower time scale, the free energy curves are synchronized.

A. Appendix

Lemma A.1. 1. Let be $\sup_{\mathcal{D}} \|a_l\|_{L^2(S, H^1(\Omega))} < \infty$ and the assumptions of Theorem 4.2 be fulfilled. Then

$$\|a_l - a_h\|_{L^2(S, L^2)} \rightarrow 0 \quad (1.31)$$

as $\text{size } \mathcal{D} \rightarrow 0$.

Proof. We decompose the integral over the whole domain into the intersected area of the control volume K and the kite D_σ (see Subsection 3.2) over the edge $\sigma = K|L$

$$\begin{aligned} T_1 &:= \|a_l - a_h\|_{L^2(S, L^2(\Omega))}^2 = \int_S \int_{\Omega} (a_l(x) - a_h(x))^2 dx dt \\ &= \int_S \sum_{K \in \mathcal{V}} \sum_{L \in \mathcal{N}_{\mathcal{V}}(K)} \int_{K \cap D_\sigma} (a_l(x) - a_K)^2 dx dt. \end{aligned}$$

Using Taylor expansion of a_l around x_K and the boundedness of the gradient we get

$$\begin{aligned} T_1 &\leq (\text{size } M)^2 \int_S \sum_{K \in \mathcal{V}} \sum_{L \in \mathcal{N}_{\mathcal{V}}(K)} \int_{K \cap D_\sigma} |\nabla a_l(x_K)|^2 dx dt \\ &\leq (\text{size } M)^2 \|a_l\|_{L^2(S, H^1(\Omega))}^2 \rightarrow 0 \end{aligned}$$

as $\text{size}(\mathcal{D}) \rightarrow 0$. □

We introduce the weak gradient reconstruction operator $\nabla_w : X_{\mathcal{V}}(\mathcal{M}) \rightarrow L^2(\Omega)^2$ by

$$\nabla_w a_l(\mathbf{x}) := 2 \frac{a_L - a_K}{d_\sigma} \mathbf{t}_\sigma \quad \text{for } \mathbf{x} \in D_\sigma, \sigma = K|L.$$

The vector \mathbf{n}_σ denotes a unit normal vector of the face $\sigma = K|L \in \mathcal{E}_{int}$, the direction is arbitrary, but fixed. Then, the vector \mathbf{t}_σ denotes the unit tangent vector of the straight line $\overline{x_K, x_L}$ which is a $-\pi/2$ rotation of \mathbf{n}_σ .

Lemma A.2. Assuming that we have a sequence $(a_l)_l$ in $L^2(S, H^1(\Omega))$ with an a-priori bound $\|a_l\|_{L^2(S, H^1(\Omega))} \leq C$, then we can extract a subsequence (also called a_l) converging to $\hat{a} \in L^2(S, H^1(\Omega))$ in the following senses

$$a_l \rightharpoonup \hat{a} \text{ in } L^2(S, H^1(\Omega)), \quad \nabla_w a_l \rightharpoonup \nabla \hat{a} \text{ in } L^2(S, L^2(\Omega)^2).$$

Proof. Since $\|a_l\|_{L^2(S, H^1)}$ is uniformly bounded, the weak gradient reconstruction of a_l is also uniformly bounded in $L^2(S, L^2(\Omega)^2)$. Therefore there exist a subsequence and a $\hat{g} \in L^2(S, L^2(\Omega)^2)$ such that $\nabla_w a_l \rightharpoonup \hat{g}$ in $L^2(S, L^2(\Omega)^2)$. We show that $\hat{g} = \nabla \hat{a}$ holds.

For this we use arbitrary test functions $\chi \in C_0^\infty(S)$ and $w \in C_0^\infty(\Omega)^2$. The set $\{g : g = \sum_{i=1}^n \chi_i w_i \text{ with } w_i \in C_0^\infty(\Omega)^2, \chi_i \in C_0^\infty(S)\}$ is dense in $L^2(S, L^2(\Omega)^2)$. According to the Helmholtz decomposition, the set $\{w : w = \nabla \varphi_c + \text{curl } \varphi_r \text{ with } \varphi_c, \varphi_r \in C_0^\infty(\Omega)\}$ is dense in $L^2(\Omega)^2$.

For all $\psi \in C_0^\infty(\Omega)$ we denote by ψ_l the Lagrange interpolant of ψ consisting in a continuous piecewise affine function such that for all nodes x_K in the mesh one obtains $\psi_l(x_K) = \psi(x_K)$. Due to regularity of the mesh, one gets from classical FEM theory $\psi_l \rightarrow \psi$ in $H^1(\Omega)$. Moreover, we introduce a strong gradient interpolation operator by

$$\nabla_s \psi(\mathbf{x}) := \frac{\psi(x_L) - \psi(x_K)}{d_\sigma} \mathbf{t}_\sigma + \frac{\psi(\mathbf{x}_{T_{\sigma K}}) - \psi(\mathbf{x}_{T_{\sigma L}})}{m_\sigma} \mathbf{n}_\sigma \quad \text{for } \mathbf{x} \in D_\sigma, \sigma = K|L,$$

where $\mathbf{x}_{T_{\sigma K}}$ and $\mathbf{x}_{T_{\sigma L}}$ denote the circumcenters of the triangles to the left and to the right of $\overline{x_K, x_L}$. Furthermore the continuous curl operator is defined by a $(-\frac{\pi}{2})$ rotation of the gradient, i.e., one has

$$\text{curl } \psi = \begin{pmatrix} \psi_y \\ -\psi_x \end{pmatrix} = - \begin{pmatrix} \psi_x \\ \psi_y \end{pmatrix}^\perp = -(\nabla \psi)^\perp.$$

Therefore, the strong curl interpolator is defined by

$$\operatorname{curl}_s \psi(\mathbf{x}) := -\frac{\psi(x_L) - \psi(x_K)}{d_\sigma} \mathbf{n}_\sigma + \frac{\psi(\mathbf{x}_{T_{\sigma K}}) - \psi(\mathbf{x}_{T_{\sigma L}})}{m_\sigma} \mathbf{t}_\sigma \quad \text{for } \mathbf{x} \in D_\sigma, \sigma = K|L.$$

Using Helmholtz decomposition we obtain

$$\widehat{g}(t) = \nabla g_r(t) + \operatorname{curl} g_c(t) \quad g_r(t), g_c(t) \in H^1(\Omega) \text{ f.a.a. } t \in S.$$

Irrotational part: First we show that the irrotational part of \widehat{g} in the sense of Helmholtz decomposition equals $\nabla \widehat{a}$. Due to the orthogonality of \mathbf{t}_σ and \mathbf{n}_σ we have

$$\begin{aligned} S &= \int_S \chi \int_\Omega \nabla a_l \cdot \nabla \varphi_{r,l} dx dt \\ &= \int_S \chi \sum_{\sigma=K|L \in \mathcal{E}_{int}} \frac{m_\sigma}{d_\sigma} (a_K - a_L) (\varphi_r(x_K) - \varphi_r(x_L)) dt \\ &= \int_S \chi \sum_{\sigma=K|L \in \mathcal{E}_{int}} |D_\sigma| \left(2 \frac{a_K - a_L}{d_\sigma} \right) \left(\frac{\varphi_r(x_K) - \varphi_r(x_L)}{d_\sigma} \right) dt \\ &= \int_S \chi \int_\Omega \nabla_w a_l \cdot \nabla_s \varphi_{r,l} dx dt. \end{aligned}$$

By weak-strong convergence, we obtain in the first and the last integral

$$\int_S \chi \int_\Omega \nabla \widehat{a} \cdot \nabla \varphi_r dx dt = \int_S \chi \int_\Omega \widehat{g} \cdot \nabla \varphi_r dx dt$$

and therefore $\nabla \widehat{g}_r(t, x) = \nabla \widehat{a}(t, x)$ f.a.a. $(t, x) \in Q$.

Divergence-free part: Now, it remains to show that the divergence-free part of \widehat{g} vanishes. In [27] it is shown that covolume discretizations on Delaunay-Voronoi grids fulfill the continuous property $\nabla \cdot \operatorname{curl} \psi \equiv 0$ in a discrete sense, which will be used in the following. For the sake of completeness, we present the necessary arguments. Obviously, we obtain for the strong curl interpolator on regular meshes $\operatorname{curl}_s \psi \rightarrow \operatorname{curl} \psi$ in $L^2(\Omega)^2$. Now we compute

$$\begin{aligned} &\int_Q \chi \nabla_w a_l \cdot \operatorname{curl}_s \varphi_c dx dt \\ &= \int_S \chi \sum_{\sigma=K|L \in \mathcal{E}_{int}} |D_\sigma| \left(2 \frac{a_L - a_K}{d_\sigma} \right) \left(\frac{\varphi_c(\mathbf{x}_{T_{\sigma K}}) - \varphi_c(\mathbf{x}_{T_{\sigma L}})}{m_\sigma} \right) dt \\ &= \int_S \chi \sum_{\sigma=K|L \in \mathcal{E}_{int}} (a_L - a_K) (\varphi_c(\mathbf{x}_{T_{\sigma K}}) - \varphi_c(\mathbf{x}_{T_{\sigma L}})) dt \\ &= \int_S \chi \sum_{\substack{L \in \mathcal{V} \\ x_L \notin \partial\Omega}} \sum_{K \in \mathcal{N}_V(L)} a_L (\varphi_c(\mathbf{x}_{T_{\sigma K}}) - \varphi_c(\mathbf{x}_{T_{\sigma L}})) dt \\ &= 0. \end{aligned}$$

The last integral is always identically 0, since we add the same term $\varphi_c(\mathbf{x}_{T_{\sigma K}})$ one times positively, and one times negatively. By weak-strong convergence of the first integral, we finally obtain

$$\int_Q \chi \widehat{g} \cdot \operatorname{curl} \varphi_c dx dt = 0,$$

i.e., the divergence-free part of \widehat{g} vanishes, and we have indeed $\widehat{g}(t, x) = \nabla \widehat{a}(t, x)$ f.a.a. $(t, x) \in Q$ and \square

Lemma A.3. Let Ω be an open, bounded polyhedral subset of \mathbb{R}^N . Moreover, let $\{\mathcal{M}\}$ be a series of Voronoi finite volume meshes with $\text{size}(\mathcal{M}) \rightarrow 0$. Let be $u \in L^\infty(\Omega)$. Then the piecewise constant functions u_h with $u_h(x) = u_K$ if $x \in K$,

$$u_K = \frac{1}{|K|} \int_K u(x) dx \quad \forall K \in \mathcal{V},$$

converge to u in $L^p(\Omega)$ for all $p \in [1, \infty)$ as $\text{size}(\mathcal{M}) \rightarrow 0$.

Proof. We show the result for $p = 1$, the assertion for $p \in (1, \infty)$ then results from

$$\|u_h - u\|_{L^p} \leq (2\|u\|_{L^\infty})^{\frac{p-1}{p}} \|u - u_h\|_{L^1}^{1/p}.$$

Let be $\varepsilon > 0$. Luzin's theorem guarantees the existence of a closed set $M_\varepsilon \subset \Omega$ such that

$$u|_{M_\varepsilon} \text{ is continuous and } \text{mes}(\Omega \setminus M_\varepsilon) < \frac{\varepsilon}{8\|u\|_{L^\infty}}.$$

Since M_ε is compact there exists a $\delta > 0$ such that

$$|u(x) - u(y)| < \frac{\varepsilon}{2 \text{mes} \Omega} \quad \forall x, y \in M_\varepsilon, |x - y| < \delta.$$

Let $\text{size}(\mathcal{M}) < \delta$ which implies $|x - y| < \delta$. Introducing the set

$$K \setminus M_\varepsilon := \{x \in \mathbb{R}^N : x \in K, x \notin M_\varepsilon\}$$

we estimate the integral in the L^1 -norm by considering integrals on subsets

$$\begin{aligned} \|u - u_h\|_{L^1} &\leq \sum_{K \in \mathcal{V}} \frac{1}{|K|} \int_K \int_K |u(x) - u(y)| dy dx \\ &= \sum_{K \in \mathcal{V}} \frac{1}{|K|} \int_{K \cap M_\varepsilon} \int_{K \setminus M_\varepsilon} |u(x) - u(y)| dy dx \\ &\quad + \sum_{K \in \mathcal{V}} \frac{1}{|K|} \int_{K \cap M_\varepsilon} \int_{K \setminus M_\varepsilon} |u(x) - u(y)| dy dx \\ &\quad + \sum_{K \in \mathcal{V}} \frac{1}{|K|} \int_{K \setminus M_\varepsilon} \int_K |u(x) - u(y)| dy dx \\ &< \frac{\varepsilon}{2 \text{mes} \Omega} \text{mes} \Omega + 2\|u\|_{L^\infty} \frac{\varepsilon}{8\|u\|_{L^\infty}} + 2\|u\|_{L^\infty} \frac{\varepsilon}{8\|u\|_{L^\infty}} = \varepsilon \end{aligned}$$

□

Lemma A.4. We assume (A2) for Ω . Let $\mathcal{D} = (\mathcal{M}, (t_\delta^{(n)})_{n=1}^N)$ be a sequence of discretizations of $Q = S \times \Omega$ and $a_h \rightarrow \hat{a}$ in $L^2(S, Y)$ as $\text{size}(\mathcal{D}) \rightarrow 0$ with $\|a_h\|_{L^\infty(S, L^\infty(\Omega, \mathbb{R}^m))} \leq R$. Moreover, let $f : \Omega \times \mathbb{R}^m \rightarrow \mathbb{R}_+$ satisfy Carathéodory condition and there exist $0 < \underline{c}, \bar{c} < \infty$ such that $\underline{c} \leq f(x, y) \leq \bar{c}$, f.a.a. $x \in \Omega$, $\forall y \in \mathbb{R}^m$. Additionally, there exists a constant $\gamma \in (0, 1]$ such that $f|_{\Omega_I} \in C^{0, \gamma}(\Omega_I \times \mathcal{B}_{\mathbb{R}^m}(0, R))$ for all $I \in \mathcal{I}$, where $\mathcal{B}_{\mathbb{R}^m}(0, R)$ denotes a ball in \mathbb{R}^m centered at 0 with radius R . Then

$$\|f_h(a_h) - f(\hat{a})\|_{L^1(Q)} \rightarrow 0 \quad \text{as } \text{size}(\mathcal{D}) \rightarrow 0.$$

Proof. For any given discretization \mathcal{D} , let

$$\Xi := \{x \in \Omega : x \in K \in \mathcal{V} \text{ with } |K \cap \Omega_I| \neq 0 \wedge |K \cap \Omega_J| \neq 0 \text{ for } I \neq J, I, J \in \mathcal{I}\}$$

with $|\Xi| \leq 2\theta \text{size}(\mathcal{M})$ for all discretizations \mathcal{D} (see also (A2)). In order to estimate

$$\begin{aligned} S_1 &= \|f_h(a_h) - f(\hat{a})\|_{L^1(\Omega)} = \sum_{K \in \mathcal{V}} \int_K \left| \frac{1}{|K|} \int_K f(y, a_h(x)) dy - f(x, \hat{a}(x)) \right| dx \\ &\leq \sum_{K \in \mathcal{V}} \int_K S_2(x) dx \end{aligned}$$

with

$$S_2(x) = \frac{1}{|K|} \int_K |f(y, a_h(x)) - f(x, \widehat{a}(x))| dy$$

we consider the cases:

- On $x \in \Omega \setminus \Xi$, we obtain

$$S_2(x) \leq \frac{c}{|K|} \int_K |a_h(x) - \widehat{a}(x)|^\gamma + |x - y|^\gamma dy \leq c|a_h(x) - \widehat{a}(x)|^\gamma + c \text{size}(\mathcal{M})^\gamma.$$

- On $x \in \Xi$, we find by using the bound \bar{c} of f the estimate $S_2(x) \leq 2\bar{c}$.

Therefore we deduce with some constant c_1 the following estimate

$$\begin{aligned} \int_S S_1 dt &\leq \int_S \left(\int_{\Omega \setminus \Xi} S_2 dx + \int_{\Xi} S_2 dx \right) dt \\ &\leq c_1 \text{size}(\mathcal{M})^\gamma + c_1 \sum_{\nu=1}^m \int_Q |a_{\nu,h} - \widehat{a}_\nu|^\gamma dx dt. \end{aligned}$$

Since $\gamma \in (0, 1]$, we apply Hölder's inequality with $q = 2/\gamma$ and $p = 2/(2 - \gamma)$ and conclude

$$\|f_h(a_h) - f(\widehat{a})\|_{L^1(Q)} \leq c_1 \text{size}(\mathcal{M})^\gamma + c_1 (T|\Omega|)^{1-\gamma/2} \|a_h - \widehat{a}\|_{L^2(S,Y)} \rightarrow 0,$$

as $\text{size}(\mathcal{D}) \rightarrow 0$. □

Acknowledgements

A. Fiebach was partially supported by the European Commission within the *Seventh Framework Programme (FP7)* MD³ “Material Development for Double Exposure and Double Patterning”.

A. Linke (project D27) and A. Glitzky (project D22) are partially supported by the DFG Research Center MATHEON *Mathematics for key technologies*.

The authors would like to thank Klaus Gärtner and Jens André Griepentrog for their assistance and for valuable discussions.

References

- [1] B. Andreianov, M. Bendahmane, and M. Saad. Finite volume methods for degenerate chemotaxis model. *J. Comput. Appl. Math.*, 235(14):4015–4031, 2011.
- [2] D. Bothe and M. Pierre. Quasi-steady-state approximation for a reaction-diffusion system with fast intermediate. *J. Math. Anal. Appl.*, 368(1):120–132, 2010.
- [3] J.J. Carberry. *Chemical and Catalytic Reaction Engineering*. Dover Books on Chemistry Series. Dover, 2001.
- [4] P. Deuffhard and F. Bornemann. *Gewöhnliche Differentialgleichungen*. Number Bd. 2 in Numerische Mathematik. de Gruyter, Germany, 2008.
- [5] R. Eymard, T. Gallouët, and R. Herbin. The finite volume method. In Philippe Ciarlet and Jean-Louis Lions, editors, *Handbook of Numerical Analysis*, pages 713–1020. North Holland, 2000.
- [6] R. Eymard, A. Handlovicova, R. Herbin, K. Mikula, and O. Stašová. Applications of approximate gradient schemes for nonlinear parabolic equations. Technical report, 2012.

- [7] R. Eymard, D. Hilhorst, H. Murakawa, and M. Olech. Numerical approximation of a reaction-diffusion system with fast reversible reaction. *Chin. Ann. Math., Ser. B*, pages 1–24, 2010.
- [8] A. Fiebach, A. Glitzky, and A. Linke. Uniform global bounds for solutions of an implicit Voronoi finite volume method for reaction-diffusion problems. Submitted to *Numer. Math.*
- [9] J. Fuhrmann, A. Fiebach, and G. P. Patsis. Macroscopic and stochastic modeling approaches to pattern doubling by acid catalyzed cross-linking. In *Proc. of SPIE*, volume 7639, page 76392I. SPIE, 2010.
- [10] J. Fuhrmann, A. Fiebach, M. Uhle, A. Erdmann, C. R. Szmanda, and C. Truong. A model of self-limiting residual acid diffusion for pattern doubling. *Microelectron. Eng.*, 86(4-6):792–795, 2009.
- [11] H. Gajewski and K. Gröger. Reaction—diffusion processes of electrically charged species. *Math. Nachr.*, 177(1):109–130, 1996.
- [12] H. Gajewski and I. V. Skrypnik. Existence and uniqueness results for reaction-diffusion processes of electrically charged species. In *Nonlinear Elliptic and Parabolic Problems (Zurich 2004)*, volume 64 of *Progress in Nonlinear Differential Equations and Their Applications*, pages 151–188. Birkhäuser, Basel, 2005.
- [13] Gärtner, K. Existence of bounded discrete steady-state solutions of the van Roosbroeck system on boundary conforming Delaunay grids. *SIAM J. Sci. Comput.*, 31(2):1347–1362, 2009.
- [14] V. Giovangigli. *Multicomponent flow modeling*. Modeling and simulation in science, engineering & technology. Birkhäuser, 1999.
- [15] A. Glitzky. Uniform exponential decay of the free energy for Voronoi finite volume discretized reaction-diffusion systems. *Math. Nachr.*, 284(17-18):2159–2174, 2011.
- [16] A. Glitzky and K. Gärtner. Energy estimates for continuous and discretized electro-reaction-diffusion systems. *Nonlinear Anal., Theory Methods Appl., Ser. A*, 70(2):788–805, 2009.
- [17] A. Glitzky, K. Gröger, and R. Hünlich. Free energy and dissipation rate for reaction diffusion processes of electrically charged species. *Appl. Anal.*, 60(3-4):201–217, 1996.
- [18] A. Glitzky and R. Hünlich. Energetic estimates and asymptotics for electro-reaction-diffusion systems. *Z. Angew. Math. Mech.*, 77(11):823–832, 1997.
- [19] A. Glitzky and R. Hünlich. Global estimates and asymptotics for electro-reaction-diffusion systems in heterostructures. *Appl. Anal.*, 66(3-4):205–226, 1997.
- [20] K. Gröger. Free energy estimates and asymptotic behaviour of reaction–diffusion processes. Preprint 20, Institut für Angewandte Analysis und Stochastik im Forschungsverbund Berlin e.V., 1992.
- [21] R. N. Hall. Electron-hole recombination in germanium. *Phys. Rev.*, 87:387–387, Jul 1952.
- [22] L.V. Kalachev, H.G. Kaper, T.J. Kaper, N. Popovic, and A. Zagaris. Reduction for Michaelis-Menten-Henri kinetics in the presence of diffusion. *Electron. J. Differ. Equ.*, Conference 16:155–184, 2007.
- [23] O.A. Ladyzhenskaya, V.A. Solonnikov, and N.N. Ural'tseva. *Linear and quasi-linear equations of parabolic type*. Translated from the Russian by S. Smith. Translations of Mathematical Monographs. 23. Providence, RI: American Mathematical Society (AMS). XI, 648 p., 1968.
- [24] C.A. Mack. *Fundamental Principles of Optical Lithography : the Science of Microfabrication*. Wiley, Chichester, West Sussex, England, 2007.

- [25] L. Michaelis and M.L. Menten. Die Kinetik der Invertinwirkung. *Biochem. Zeitsch.*, 49:333–369, 1913.
- [26] D. L. Nelson and M. M. Cox. *Lehninger Principles of Biochemistry, Fourth Edition*. Fourth edition edition, 2004.
- [27] R. A. Nicolaides. Direct discretization of planar div-curl problems. *SIAM J. Numer. Anal.*, 29(1):32–56, 1992.
- [28] M. Pierre. Global existence in reaction-diffusion systems with control of mass: a survey. *Milan J. Math.*, 78(2):417–455, 2010.
- [29] O. Schenk and K. Gärtner. Solving unsymmetric sparse systems of linear equations with PARDISO. In *Computational science—ICCS 2002, Part II (Amsterdam)*, volume 2330 of *Lecture Notes in Comput. Sci.*, pages 355–363. Springer, Berlin, 2002.
- [30] O. Schenk and K. Gärtner. On fast factorization pivoting methods for sparse symmetric indefinite systems. *ETNA, Electron. Trans. Numer. Anal.*, 23:158–179, 2006.
- [31] L. A. Segel and M. Slemrod. The quasi-steady state assumption: a case study in perturbation. *SIAM Rev.*, 31(3):446–477, September 1989.
- [32] J. R. Shewchuk. Triangle: Engineering a 2D Quality Mesh Generator and Delaunay Triangulator. In Ming C. Lin and Dinesh Manocha, editors, *Applied Computational Geometry: Towards Geometric Engineering*, volume 1148 of *Lecture Notes in Computer Science*, pages 203–222. Springer-Verlag, May 1996. From the First ACM Workshop on Applied Computational Geometry.
- [33] W. Shockley and W. T. Read. Statistics of the recombinations of holes and electrons. *Phys. Rev.*, 87:835–842, Sep 1952.